# TRAPPING AND IDENTIFICATION OF OXIDIZED MERCURY SPECIES IN FLUE GAS

Edwin S. Olson, Jeffrey S. Thompson, John H. Pavlish

Energy and Environmental Research Center, University of North Dakota

Grand Forks, ND 58202

**KEY WORDS:** mercury measurement, speciation, gas chromatography–mass spectrometry

## ABSTRACT

Current methods for speciation of vapor-phase mercury do not distinguish the inorganic forms of oxidized mercury. The assumption that Hg(II) is $HgCl_2$ or HgO for modeling behavior of oxidized mercury is unwarranted. Advances in cryogenic and solvent trapping of oxidized mercury species and their analysis by mass spectrometry led to the conclusion that surface reactions of elemental mercury with flue gas components result in more complex chemistry. Recent research demonstrated that in a simulated flue gas stream containing $NO_2$ and $SO_2$, the volatile form of the mercury emitted from the sorbent after breakthrough was determined to be mercury (II) nitrate hydrate, $Hg(NO_3)_2 \cdot H_2O$. Improvements in the sampling and analysis allowed for examination of other reaction products. Mercuric chloride and mercuric nitrate hydrate are separated by gas chromatography and identified by mass spectrometry. The eventual goal of this effort is a definitive speciation technique for determination of oxidized mercury in combustion flue gas.

## INTRODUCTION

Much attention is currently focused on the air emission of trace amounts of toxic inorganic compounds during combustion of fossil fuels and incineration of waste materials. Mercury is of particular interest, owing to the high volatility of mercury and certain mercury compounds, the biological pathways that result in its concentration in fatty tissues, and its potential neurotoxic effect. To understand the complexities of its emission during combustion and dispersion throughout the environment, it is necessary to identify the mechanisms for its transformations, including capture on sorbents, scrubbers, or other control devices and release from these devices. Understanding these mechanism in turn requires identification and quantitation of the forms of mercury compounds involved. Previous and ongoing identifications or speciations of trace mercury are based mainly on distinguishing oxidized from elemental mercury forms. Often it is assumed that oxidized mercury in the gas phase is mercuric chloride, since that is the most well-known volatile mercury salt. Predictions based on this *implicit speciation* could be erroneous if one uses the thermodynamic stabilities of mercuric chloride to represent the behavior of oxidized mercury.

Characterization of trace amounts of solid-phase mercury has progressed further, especially with the application of XAFS. Mercury forms sorbed on three types of activated carbon sorbents were recently examined (1). The results for mercury chemisorbed on a lignite-derived activated carbon were consistent with a form with either a mercury–sulfur bond or a mercury–chlorine bond. This more *explicit speciation* is valuable in determining the nature of the sorption reactions.

For understanding mercury transformations between the gas and solid phases, a *definitive speciation* of mercury compounds is needed. Perhaps HgO could form in certain atmospheric conditions as a combustion gas cools, but it is unlikely that HgO desorbs from a solid phase, since the heat required to decouple the mercury–oxygen bonds in the polymer is too high; thus elemental mercury is more likely released. That simply points to a need for a method to identify not only HgO in the gas phase but also many other mercury species containing nitrogen, sulfur, oxygen, and chlorine.

Previous research at the Energy & Environmental Research Center (EERC) was successful in cryogenically trapping oxidized mercury forms from a gas stream (2). Selective desorption could separate elemental mercury from oxidized forms, but the desorption of oxidized forms was not accompanied by a selective identification method.

Recently, the EERC reported the trapping and identification of the oxidized mercury species that is released from an activated carbon sorbent after breakthrough in a simulated flue gas stream containing both $SO_2$ and $NO_2$ ( 3 ). In an extensive matrix of mercury sorption experiments with flue gas components (4), early breakthrough was observed only when $NO_2$ and $SO_2$ were both present in the gas phase. Many years ago, the reaction of $NO_2$ with Hg was shown to form HgO on the container surface (5). This reaction is consistent with the high sorption capacity observed on carbons

in a gas containing $NO_2$ and not $SO_2$. Later, Freeman and Gordon (6) presented evidence for mercurous nitrite and mercurous nitrate in solid products from the reaction. To understand the early breakthrough interaction when $SO_2$ is added to experiments, identification of the volatile oxidized mercury species was required. This was established by trapping the effluent gas in a cold organic solvent, evaporating part of the solvent, and analyzing by GC–MS. This high-confidence technique demonstrated that the released mercury product formed in the $NO_2$–$SO_2$ mixture was mainly mercuric nitrate hydrate (3). Both $MnO_2$ and catalytic carbons behaved similarly.

In other environments, species such as $HgCl_2$ could also be present and detectable. Work in an earlier CATM project established that $HgCl_2$ could be trapped cryogenically and subsequently desorbed readily as an oxidized mercury species, presumed to be the original $HgCl_2$ (2).

Transformations of the oxidized species in the flue gas to other oxidized species are anticipated as a result of gas-phase or gas–solid reactions. Methods for distinguishing these species, mixtures of these species, and other oxidized species are needed to understand the interactions occurring on sorbents, ash particles, and duct or filter bag surfaces.

Whether other oxidized mercury species are present in sorbent breakthrough emission or flue gas emissions in general is unknown. It is important to determine the definitive speciation of all emitted oxidized species in order to understand the reactions that occur on the sorbent that lead to inferior mercury sorbent performance in flue gas component mixtures. These interactions between mercury and gas components are also very important in understanding speciation of mercury in combustion flue gases and similar interactions that may occur on ash particles.

Organomercury compounds, as well as $HgCl_2$, have been separated and determined by GC; however, the trapping and identification of a nonhalogenated vapor-phase oxidized mercury species is a novel breakthrough in mercury research. The goal of present research is to develop cryogenic trapping and desorption methods for oxidized mercury species and to develop and apply high-confidence MS methods for identification and quantitation of oxidized mercury species.

## RESULTS

In order to develop a method for determination of oxidized mercury compounds in the gas phase by cryogenic trapping coupled with desorption into a GC–MS, the volatility and stability of the mercury compounds of interest must be understood. The volatility behavior of mercuric chloride is better known, and the application to trapping and desorption appeared straightforward (2). Other mercury salts are less well understood. A recrystallized standard of $Hg(NO_3)_2 \cdot H_2O$ was prepared and vaporized in a gas flow as a source of $Hg(NO_3)_2 \cdot H_2O$ vapor. The gas flow was trapped cryogenically, and the concentration was determined by desorption, conversion to elemental mercury in a heated tube, and detection with a conventional atomic fluorescence spectrometer. This gave reproducible peak area responses. This established that a constant source for vapor phase $Hg(NO_3)_2 \cdot H_2O$ could be utilized for loading traps with this species and that trapping and desorption of this compound are feasible.

Conditions for GC–MS analysis of $HgCl_2$–$Hg(NO_3)_2 \cdot H_2O$ mixtures were investigated. Previous studies indicated that acetonitrile solutions of $Hg(NO_3)_2 \cdot H_2O$ could be injected in a standard inlet operated under splitless conditions, and the $Hg(NO_3)_2 \cdot H_2O$ eluted as a fairly sharp peak at 5.4 minutes through a nonpolar (DB5) 30-meter column. A unique mass spectrum corresponding to $Hg(NO_3)_2 \cdot H_2O$ was observed for this peak. Injection of $HgCl_2$ in acetonitrile resulted in elution of a $HgCl_2$ peak with its characteristic mass spectrum. The $HgCl_2$ peak eluted later than the $Hg(NO_3)_2 \cdot H_2O$ and was very broad. This indicates that $HgCl_2$ interacts much more strongly with the column phase than does $Hg(NO_3)_2 \cdot H_2O$, as one would expect.

During the chromatography of $Hg(NO_3)_2 \cdot H_2O$, some elemental mercury forms in the GC injector from decomposition of the $Hg(NO_3)_2 \cdot H_2O$ on the injector surfaces and elutes very early in the chromatogram. It is also likely that some mercury is vented from the inlet. Thus the response for $Hg(NO_3)_2 \cdot H_2O$ is not as high as hoped, but standard injection in a solvent is probably not the ideal way to introduce these compounds to the mass spectrometer. In fact, the injection temperature had to be lowered to get a better response for the $HgCl_2$. Except for the elemental, no other Hg-containing peaks, such as an acetonitrile complex or product resulting from decomposition, were observed.

When mixtures of $Hg(NO_3)_2 \cdot H_2O$ and $HgCl_2$ in acetonitrile were injected at an intermediate temperature, two peaks were observed at their characteristic retention times in the chromatogram (Figure 1b). Reconstructed selected ion chromatograms for the isotopic cluster at m/z 250–254 representing the $Hg(NO_3)_2 \cdot H_2O$ peak and at m/z 270–274 representing the $HgCl_2$ peak are shown

in Figures 1c and 1d, respectively. The mass spectrum of $Hg(NO_3)_2 \cdot H_2O$ representing one scan in the $Hg(NO_3)_2 \cdot H_2O$ peak is shown in Figure 1a. The base peak is at m/z 252 with a characteristic pattern for the mercury isotope ions (3). The molecular ion is very small for this compound and cannot be seen in the mass spectrum for this scan.

While it is clear that optimization of the inlet configuration and chromatography conditions are needed, these experiments establish the feasibility of observing at least two oxidized mercury species as they elute from a GC column. These two compounds appear to have no difficulty transferring through the coated columns that are necessary to maintain the vacuum conditions. Of course, other mercury compounds may not survive inlets, columns, or desorption conditions and may convert to these and other species.

Replacement of the standard GC inlet with a 1-mL glass vial for introducing oxidized mercury species was investigated. The vial was fitted with a small septum through which an inlet capillary (from the injector assembly) and outlet capillary (the GC column) were inserted through the septum. The vial was loaded with a mixture of $HgCl_2$ and $Hg(NO_3)_2 \cdot H_2O$ by injecting 1$\mu$L of the standard acetonitrile solution of $HgCl_2$ and $Hg(NO_3)_2 \cdot H_2O$ and allowed to evaporate for a minute. The septum cap was replaced and the vial placed in the GC oven. The GC oven temperature program was initiated and mass spectral data accumulated. The $HgCl_2$ and $Hg(NO_3)_2 \cdot H_2O$ were successfully desorbed from the vial into the column. Initially, a very short column (3 meter) was used, and both mercury compounds desorbed and eluted into the MS in a broad unresolved peak The spectra of both the $HgCl_2$ and $Hg(NO_3)_2 \cdot H_2O$ were evident, but the ion trap was not operating under high vacuum with the short column, so the spectra and reconstructed chromatogram were noisy, owing to excessive space charging. Use of a longer column resolved the peaks and allowed a better vacuum resulting in better spectra. The peaks were not as sharp as those obtained with a normal GC injector.

The vial was then loaded from a gas stream containing $Hg(NO_3)_2 \cdot H_2O$. The vial was cooled in an ice salt bath, and the $Hg(NO_3)_2 \cdot H_2O$ was loaded using the source described above. The vial was then transferred to the GC oven and attached to the column as described above with the septum cap. Again, the $Hg(NO_3)_2 \cdot H_2O$ peak was observed in the accumulated mass spectal data. Some decomposition to elemental mercury was evident. The reproducibility of this method has not yet been established, and further research in materials and techniques is needed. Of major concern is how to deal with trapped moisture that is eluted into the MS.

## CONCLUSION

GC–MS methods were used to separate a mixture of two volatile oxidized mercury species, $HgCl_2$ and $Hg(NO_3)_2 \cdot H_2O$, and give characteristic mass spectra for the two components. The separation and analysis can occur with materials trapped from the gas phase into a solvent and subsequent injection into the GC–MS injection port or by desorption from a solid phase in a small trapping vial. Thus definitive identification and quantitation of these two species are feasible. Present efforts are focused on developing coupling hardware for interfacing larger traps to the GC–MS.

## ACKNOWLEDGMENTS

The authors express their thanks to the following sponsors: North Dakota Industrial Commission; EERC Center for Air Toxic Metals Program sponsored by EPA under Assistance Agreements CR821518k CR823173, and CR824854; Otter Tail Power Company; and Northern States Power Company.

## REFERENCES

1. Huggins, F.E.; Huffman, G.P.; Dunham, G.E.; Senior, C.L. *Energy & Fuels* **1999**, *13*, 114.
2. Thompson, J.S.; Pavlish, J.H. Cryogenic Trapping of Oxidized Mercury Species from Combustion Flue Gas. *Proceedings of the Air Quality Conference*; McLean, VA, Dec 1, 1998.
3. Olson, E.S.; Sharma, R.K.; Miller, S.J. Dunham, G.E. Mercury in the Environment. *Proceedings of a Specialty Conference*; VIP-91, Air & Waste Manag. Assoc., Minneapolis, MN, Sept. 15, 1999, p. 121.
4. Miller, S.J.; Dunham, G.E.; Olson, E.S. Mercury Sorbent Development for Coal-Fired Boilers. *Proceedings of the Air Quality Conference*, McLean, VA, Dec 1, 1998.
5. Pierce, W.C.; Noyes, W.A. *J. Amer. Chem. Soc.* **1928**, *50*, 2179.
6. Freeman, E.S.; Gordon, S. *J. Amer. Chem. Soc.* **1956**, *78*, 1813.

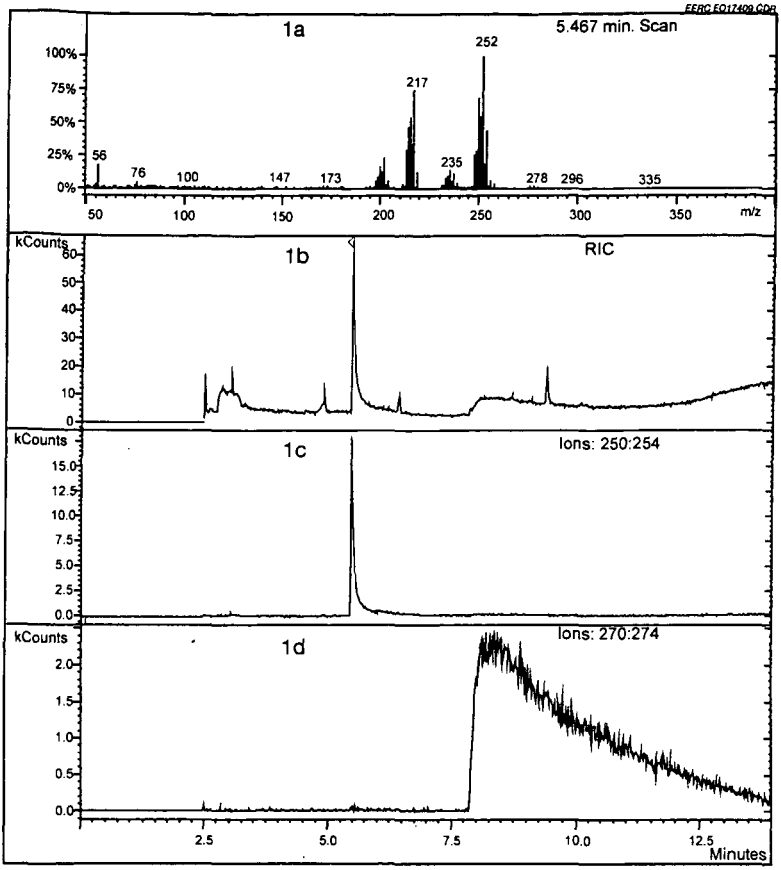


Figure 1a. Mass spectrum for Scan 329; 1b, total in chromatogram; 1c, selected ion chromatogram for m/z 250-254; and 1d, selected ion chromatogram for m/z 270-274.

# ANALYSIS OF HIGH TEMPERATURE COHESION OF ASH PARTICLES USING MODEL PURE SILICA POWDERS COATED WITH ALKALI METALS

Hidehiro Kamiya, Akira Kimura, and Makio Naito*

Graduate School of Bio-Application System Engineering, BASE, Tokyo University of Agriculture & Technology, Koganei, Tokyo 184-8588, Japan
* Japan Fine Ceramics Center, Atsuta-ku, Nagoya Japan

**ABSTRACT.** This paper analyzes the mechanism of increasing cohesive behavior of ash powders at elevated temperatures. Model ash powders were prepared from fine pure silica powder coated on the surface with 0.5 wt% alkali metal. The cohesive behavior and deformation properties of model ash powder beds were determined by using a new split type tensile strength tester of powder beds. The behavior of fly ash collected in pulverized coal combustion and model ash powders were compared. In the high temperature range above 1100 K, a rapid increase of tensile strength and plastic deformation of the ash powder beds occurred in both the natural ash and the model silica particles. It is suggested that the coated alkali metal on the silica powders reacted with the amorphous silica phase and formed a small amount of low melting point eutectic materials.

## INTRODUCTION

The increase of stickiness and adhesion force of ash powder at high temperatures hinders the stable operation and scale-up design of various high efficiency coal combustion power generation system, for example, the integrated coal gasification combined cycle (IGCC) and pressurized fluidized bed combustor (PFBC) systems. Dry ash particle deposition and the growth of a deposited ash layer on the water-cooled wall blocked the gasifier in IGCC systems and pulverized-coal combustors[1]. In PFBC systems, the operation of filter cake detachment on rigid ceramic filters by reverse-pulsing has difficulty with the increase of the adhesive force of ash[2]. These cohesive properties of ash particles at these high temperatures depend on many physical and chemical factors.

In our previous paper we measured the tensile strength of fly ash powder beds by using a diametal compression test of ash powder pellets[3] and a new split type tensile strength tester of ash powder beds[4] at high temperature at a range from room temperature to 950°C. We reported that the tensile strength of ash powder beds rapidly increased over a range of 800°C.

This paper analyzes the mechanism of increasing cohesive behavior of ash powders at elevated temperatures by using model ash powders, which were prepared from fine pure silica powder coated on the surface with 0.5 wt% alkali metal. The cohesive behavior and deformation properties of model ash powder beds were determined by using a new split type tensile strength tester of powder beds. Based on the comparison with these results of fly ash and model powders, the increasing mechanism of ash powder stickiness at high temperature is discussed.

## EXPERIMENTAL PROCEDURE

### Model ash powder preparation and characterization

The original powder samples used a commercial pure fused amorphous silica powder and fly ash. Fly ash powder was collected in a commercial pulverized coal combustion plant. The chemical component and particle size distribution of each sample were determined using ICP and a

centrifugal sedimentation method shown in Table 1. The total impurity such as Na, K, etc. in the high-pure amorphous silica powder was about 13 ppm. The concentration of sodium and potassium in the fly ash was about 0.5%. The mean particle diameter of each sample was similar at about 5 μm.

**Table 1 Mean diameter and chemical component of pure silica and fly ash powders**

| Powder sample | Mean diameter | Chemical component [wt%] | | | | |
|---|---|---|---|---|---|---|
| | | $SiO_2$ | $Al_2O_3$ | $Fe_2O_3$ | $K_2O$ | $Na_2O$ |
| Pure silica | 5.3 μm | 99.99 | 13 ppm | | | |
| Fly ash | 4.75 μm | 45.0 | 38.5 | 4.6 | 0.3 | 0.5 |

Based on the above results, model ash powders were prepared from a commercial pure fused silica powder. Firstly, pure silica powder was added to the sodium or potassium oxalate solution. The amount of silica particles added and the concentration of the oxalate solution was adjusted so that the alkali metal concentration would become 0.5 wt% (silica) after drying. The silica suspension was mixed for one minute by a planetary type mixer and dried in an oven at 120°C. After grinding with a pestle and mortar, dried silica powders with alkali oxalate were heat treated at 620°C for 1 hour, causing thermal decomposition and removal of the oxalate.

### Split type tensile strength tester for powder beds

The detail of a sprit type tensile strength test at high temperatures was described in our previous paper[4]. The powders were placed in a circular cell 5 cm in diameter with a depth of 1 cm. The cell can be divided equally into a stationary and a movable part; both parts were prepared with high-purity silica glass. After fixing the mobile part using a hook, powder samples were packed into the cell and consolidated by uni-axial pressing (2.5 kPa for 600 s). Tensile testing was carried out at various temperatures ranging from room temperature to 1173 K, with an electric furnace at a heating rate of 600°C/h. After heat treatment at each temperature for 540 s before the tensile test, the hook used to fix the mobile cell is removed, and the mobile cell is pulled in each high temperature conditions. The relationship between load and displacement during loading was then measured.

## RESULTS AND DISCUSSION

### Tensile strength and deformation behavior of fly ash and pure fused silica

Examples of tensile load and displacement relationship at room temperature and 1123 K are shown in Fig. 1. The brittle failure of both powder beds was observed after elastic deformation at room temperature. In the case of the pure silica powder sample, the brittle failure of the powder bed appeared at 1073 K. On the contrary, in the case of fly ash samples, viscous deformation appeared near the maximum load at 1073 K. Under conditions of relatively low temperatures below 1000 K, the adhesive force of both powders increased gradually in proportion to temperature. The tensile strength of the pure silica powder bed gradually increased, even in elevated temperatures (> 1073 K). However, a rapid increase of tensile strength of fly ash powder beds was observed in the high temperature range (> 1073 K).

### Model ash powders

To analyze this rapid increasing tensile strength of fly ash above 1100 K, the relationship between tensile strength and deformation behavior of alkali metal coated pure silica powder beds with

different coating condition at different temperature were measured and shown in Fig. 2. The rapid increase of tensile strength with viscous tensile deformation was observed by a coating of 0.5 % alkali metal on the surface of pure silica powders in a high temperature range above 1073 K.

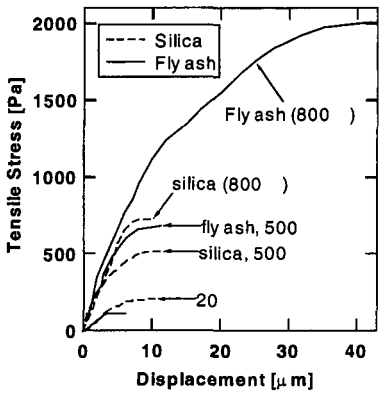


Fig. 1. Examples of tensile stress and displacement relationship of ash and silica.

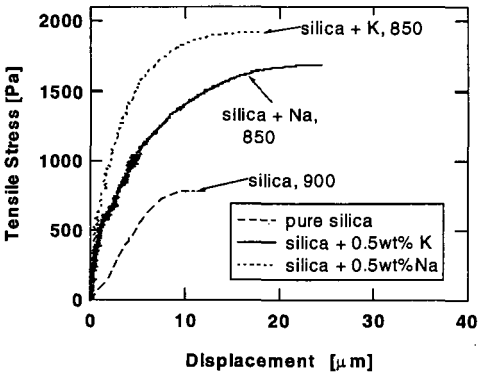


Fig. 2. An example of the tensile stress and displacement relationship of model ash powder beds prepared from pure amorphous silica powder and alkali metals.

The effect of testing temperature on the tensile strength of model ash powder beds with different alkali coating conditions is shown in Fig. 3. Regardless of the alkali metal used, the tensile strength of the model powder beds exhibited an increase with a temperature rise above 1073 K equal to that shown in the fly ash samples. This indicates that the coated alkali metal on the silica powders reacted with the amorphous silica phase and formed a small amount of low melting point eutectic materials. Hence, above 1073 K, a small amount of liquid phase formed between silica particles consisting of amorphous silica and alkali metal. It is suggested that a small amount of low melting point eutectic materials, consisting of amorphous silica and alkali metal, formed a liquid phase and this was responsible for the majority of the increase in the adhesive force mechanism of the ash powders at high temperature. This liquid phase mix was estimated from the increase in rupture displacement during tensile test of powder beds at high temperature.

## CONCLUSION

Model ash powders prepared from pure amorphous silica powder and coated alkali metal were used to reproduced the rapid increasing tensile strength of ash particle stickiness and deformation behavior in high temperatures above 1073 K. We suggest that low melting point eutectic materials consisting of amorphous silica and alkali metal formed a small amount of liquid phase between particles and promoted the increase of ash adhesion behavior.

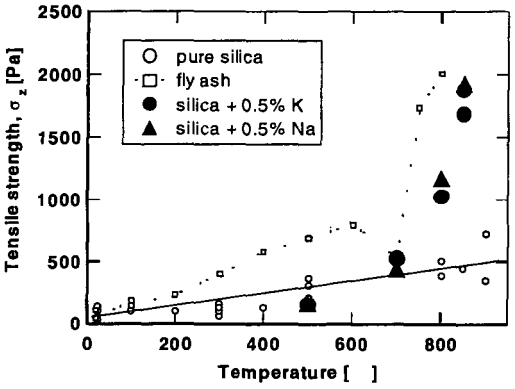


Fig. 3. The effect of temperature on tensile strength of model ash powders prepared from pure amorphous silica powders coated with sodium and potassium

**Acknowledgment**: This work is supported by the Proposal-Based New Industry Type Technology R&D Promotion Program from NEDO of Japan and Grant-in-Aid for Scientific Research (B), Japan.

## REFERENCE

1. D.H. Smith, G.J. Haddad and M. Ferer : Energy & Fuel, 11, 1006-11 (1997)
2. H. Kamiya, K. Deguchi, J. Gotou and M. Horio : "High Temperature Gas Cleaning II" p. 111-118 (1999)
3. H. Kamiya, A. Kimura, M. Horio, J.P.K. Seville and E. Kauppinen : J. of Chem. Eng. Jpn., accepted.
4. H. Kamiya, A. Kimura, T. Yokoyama, M. Naito and G. Jimbo : Pow. Tech., to be submitted.

# STUDY OF VANADIUM EMISSION CONTROL IN COMBUSTION SYSTEMS BY THERMODYNAMIC EQUILIBRIUM ANALYSES

Chang-Yu Wu and Sang-Rin Lee
University of Florida, Dept. of Environmental Engineering Sciences, Gainesville, FL 32611-6450

**Key Words:** Vanadium, Sorbent, Thermodynamic Equilibrium

## INTRODUCTION

Toxic metal emissions from combustion sources such as vanadium are of great concerns. It is concentrated in certain types of coal, heavy oil and petroleum coke[1,2]. Once emitted, it can be transported to distance, resulting in adverse environmental and health effects[3]. It is known that vanadium may cause cardiovascular disease, bronchitis and lung carcinoma. Due to its high concentration, interest has been developed to recover vanadium from ash[4]. Vanadium, as other metals in the fuel matrix, may enter the gas stream in combustion systems by vaporization or entrainment of vanadium compounds. At high temperatures, it undergoes various chemical reactions to form various species depending on the combustion environment and composition in the system. At the cooler post combustion zone, various aerosol dynamics proceed resulting in the transformation of vanadium into particulate phase. The particle size distribution depends on the temperature history and the existing species in the system[5]. A lot of research studies have shown that metals undergoing this pathway generally form aerosols in the submicrometer regime. Unfortunately, traditional control devices have their minimum efficiency in this size regime. Thus, it is important to develop new techniques to effectively control vanadium emission.

Recently, studies have been conducted to use mineral sorbents to capture heavy metals. Heavy metals are chemically adsorbed on the injected sorbent particles. As these sorbent particles are relatively larger in size (typically greater than 10 μm), the metal-sorbent particles can be easily collected using traditional particulate control devices. Shadman and co-workers[6,7] used silica, alumina and various naturally available materials (i.e. bauxite, kaolinite and lime) to capture lead and cadmium. Venkatesh et al.[8] evaluated various mineral sorbents constituting a spectrum of alumino-silicate compounds for immobilization of several heavy metals. Biswas and co-workers[9-11] *in-situ* generated sorbents particles with very high surface area to capture lead and mercury. However, no study using sorbents to capture vanadium has been conducted.

At high temperatures, reactions are fast and equilibrium can possibly be achieved. Hence thermodynamic equilibrium methods can be applied to determine the potential sorbent materials. The objective of this study is to use equilibrium calculations to determine the effective materials that can chemically adsorb vanadium. Optimal conditions to achieve high efficiencies will be determined. The impact of various common constituents in combustion systems on the performance will be assessed. The most effective one for vanadium control will be determined.

## METHODOLOGY

A computer code, STANJAN[12], was used to implement the calculations. Its principle is to minimize the system's Gibbs free energy by using the method of elemental potentials combined with atom constraints. The thermodynamic data for all the relevant species were obtained from the literature[13,14]. Table 1 lists the species that are included in the calculations. The simulation conditions are listed in Table 2. The concentrations correspond to the levels found in a typical coal combustion system[15]. Due to the lack of coal's thermodynamic data, methane ($CH_4$) is used in the calculations. As the metal concentration is trace in the fuel, the form of the fuel used in the system does not affect the metal's speciation.

Calculations were first conducted to determine the behavior of vanadium in a typical combustion system without sorbent as the baseline. The performance of individual sorbent was then investigated for a wide range of temperatures. Parametric analyses were then conducted to evaluate the impact of chlorine and sulfur. Finally, all the sorbents were included and competition for vanadium among the various sorbents was placed to determine the best sorbent.

Table 1. List of Species used in the Equilibrium Calculation

| Reactant | Product |
|---|---|
| V | V, $VCl_2$, $VCl_3$, $VCl_4$, VO, $VO_2$, $VOCl_3$,$V_2C$, $VCl_4$, $V_2O_3$, $V_2O_4$, $V_2O_5$, V(g), $VCl_2$(g), $VCl_4$(g), VO(g), $VOCl_3$(g), $VO_2$(g) |
| Ca | $CaCl_2$, CaO, $CaO_2$, $CaSO_3$, $CaSO_4$, CaS, $CaCO_3$, **$Ca(VO_3)_2$**, **$Ca_2V_2O_7$**, **$Ca_3(VO_4)_2$**, Ca(g), $CaCl_2$(g), CaS(g) |
| Mg | Mg, $Mg(OH)_2$, $MgCO_3$, $MgCl_2$, MgO, $MgSO_4$, **$Mg(VO_3)_2$**, **$Mg_2V_2O_7$**, Mg(g), $MgCl_2$(g), MgOH(g) |
| Na | Na, NaCl, NaOH, $NaClO_4$, $NaHCO_3$, $Na_2CO_3$, $Na_2O$, $Na_2O_2$, $Na_2SO_3$, $Na_2SO_4$, **$NaVO_3$**, **$Na_3VO_4$**, **$Na_4V_2O_7$**, Na(g), NaCl(g), NaOH(g), $Na_2O_2H_2$(g), $Na_2SO_4$(g) |
| Common compound | $CH_4$, CO, $CO_2$, , Cl, HCl, HOCl, NOCl, ClO, $Cl_2$, H, OH, $H_2O$, N, NO, $NO_2$, $N_2$, $N_2O$,O, $O_2$, S, $SO_2$, $SO_3$, |

Table 2. Simulation conditions for evaluating the performance of various sorbents in capturing vanadium (unit: mole).

| Set. | V | Cl | S | $CH_4$ | $O_2$ | $N_2$ | $Na_2O$ | $CaCO_3$ | MgO |
|---|---|---|---|---|---|---|---|---|---|
| I-1 | $7x10^{-7}$ | 0 | 0 | 1 | 4 | 15 | 0 | 0 | 0 |
| I-2 | $7x10^{-7}$ | 0.011 | 0 | 1 | 4 | 15 | 0 | 0 | 0 |
| II-1 | $7x10^{-7}$ | 0 | 0 | 1 | 4 | 15 | $4.12x10^{-4}$ | 0 | 0 |
| II-2 | $7x10^{-7}$ | 0 | 0 | 1 | 4 | 15 | 0 | 0.0034 | 0 |
| II-3 | $7x10^{-7}$ | 0 | 0 | 1 | 4 | 15 | 0 | 0 | $9.95x10^{-4}$ |
| III-1 | $7x10^{-7}$ | 0.011 | 0.0389 | 1 | 4 | 15 | $4.12x10^{-4}$ | 0 | 0 |
| III-2 | $7x10^{-7}$ | 0.011 | 0.0389 | 1 | 4 | 15 | 0.0778 | 0 | 0 |
| III-3 | $7x10^{-7}$ | 0.011 | 0.0389 | 1 | 4 | 15 | 0.0934 | 0 | 0 |
| III-4 | $7x10^{-7}$ | 0.011 | 0.0389 | 1 | 4 | 15 | 0 | 0.0034 | 0 |
| III-5 | $7x10^{-7}$ | 0.011 | 0.0389 | 1 | 4 | 15 | 0 | 0.0389 | 0 |
| III-6 | $7x10^{-7}$ | 0.011 | 0.0389 | 1 | 4 | 15 | 0 | 0.0467 | 0 |
| III-7 | $7x10^{-7}$ | 0.011 | 0.0389 | 1 | 4 | 15 | 0 | 0 | $9.95x10^{-4}$ |
| III-8 | $7x10^{-7}$ | 0.011 | 0.0389 | 1 | 4 | 15 | 0 | 0 | 0.0389 |
| III-9 | $7x10^{-7}$ | 0.011 | 0.0389 | 1 | 4 | 15 | 0 | 0 | 0.0467 |
| IV-1 | $7x10^{-7}$ | 0 | 0 | 1 | 4 | 15 | 0.0389 | 0.0389 | 0.0389 |
| IV-2 | $7x10^{-7}$ | 0.011 | 0.0389 | 1 | 4 | 15 | $4.12x10^{-4}$ | 0.0034 | $9.95x10^{-4}$ |
| IV-3 | $7x10^{-7}$ | 0.011 | 0.0389 | 1 | 4 | 15 | 0.0389 | 0.0389 | 0.0389 |

## RESULTS AND DISCUSSIONS

***Set I : Vanadium in a Typical Coal Combustion System Without Sorbents Added.***

In the first set, the behavior of vanadium in a typical combustion system is studied. The results are shown in Figure 1. As shown, the major product is divanadium pentaoxide ($V_2O_5$) over the entire range studied. Metal oxide aerosols formed in combustion systems are generally in the submicrometer range and hence they are not desired.[17]

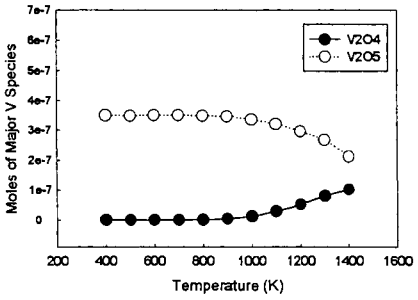


Figure 1 Partition of vanadium speciation in a typical coal combustion system without chlorine

Chlorine is known to have a strong affinity to react with many metals Therefore, its effect on vanadium speciation is also studied. The results are shown in Figure 2. As shown, vanadium oxytrichloride ($VOCl_3$) is important at medium temperatures (~500 – 1000 K) although not dominant. Compared with earlier studies on other heavy metals[5], chlorine's affinity to react with vanadium is relatively weak. Hence, it is probable that the presence of chlorine in typical combustion systems will not significantly affect vanadium's speciation.

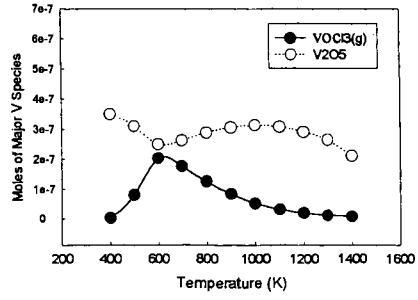


Figure 2 Partition of Vanadium species in a typical coal combustion system with chlorine

Although sulfur has been reported to be important for certain metals[5,16], calculations were not conducted in this study as there is no thermodynamic data available for vanadium-sulfur compounds.

***Set II. Performance of Individual Sorbent.***

Next, individual sorbent is examined for its performance. The amount of each sorbent used corresponds to the level found in typical coal. The results are shown in Figures 3a – 3c. As shown, all the sorbent materials used are very effective in almost the entire temperature range (forming sorbent-vanadium products). This indicates the high potential of using these materials. However, it should be noted that it does not necessarily guarantee the success of the process because of the influence by other constituents in the system. This will be discussed more in the next section.

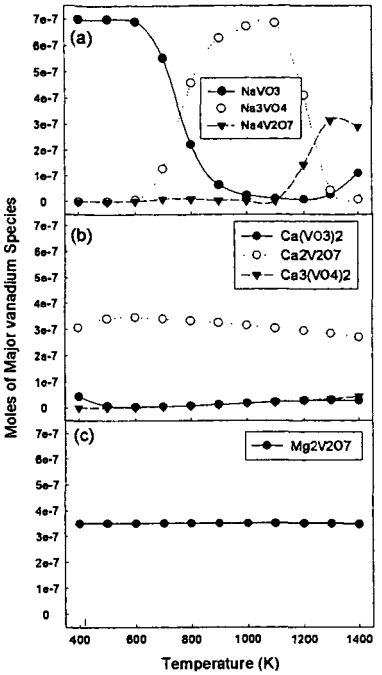


Figure 3 Partition of vanadium species using: (a) Na- based sorbent; (b) Ca-based (b) sorbent; (c) Mg-based sorbent

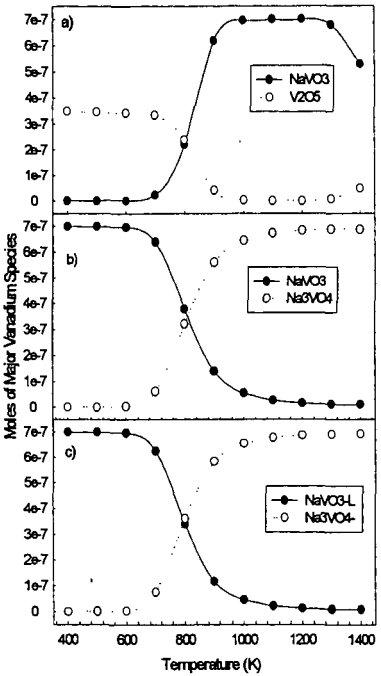


Figure 4 Impact of chlorine and sulfur on the effectiveness of Na-based sorbent: a) typical concentration in coal; b) stoichiometric amount of sorbent; c) to react with Cl and S 20% excess of sorbent than the stoichiometric amount

***Set III Effects of Chlorine and Sulfur on the Performance of the Various Sorbent Used***

Chlorine and sulfur are very common in coal and other fuels. They may react with vanadium to form vanadium chloride or sulfate. They can also react with the sorbent materials, for example, calcium sulfate (gypsum), thus reducing the available amount of sorbents to react with vanadium. Hence, their impact is investigated. First, calculations were performed using their concentrations in typical coal (Table 3). Then the stoichiometric amount necessary for scrubbing sulfur was used. Finally, 20% more of the sorbent than the stoichiometric amount was used. The results are shown in Figures 4 – 6 for Na-, Ca-, and Mg- based sorbent respectively.

**Na-based sorbent**

Figure 4a shows that $V_2O_5$ is dominant at lower temperatures (< 800K), indicating the ineffectiveness of the process. Examination of the products shows that the majority of sodium forms sodium sulfate ($Na_2SO_4$), thus depleting the available sodium. When $Na_2SO_4$ becomes unstable at higher temperatures (>900K), the sorbent is available again to react with vanadium. When the amount of sorbent is enough to deplete sulfur and chlorine, this process is effective (forming vanadium sorbent compound) even at lower temperatures, as shown in Figures 4b when stoichiometric amount of sorbent reacting with chlorine and sulfur is used.

**Ca- based sorbent**

Similar to the sodium case, Ca- based sorbent is ineffective at lower temperatures (< 1000K, Figure 5a). $V_2O_5$ is the dominant species and the cause is the same. When stoichiometric amount of calcium sorbent is used (Figure 5b), the temperature range for effective vanadium capture expands but $V_2O_5$ is still not captured effectively when the temperature is lower than 800 K. Only when excess sorbent is used (Figure 5c), calcium vanadate becomes the dominant species.

**Mg- based sorbent**

The similar trend is observed when Mg-based sorbent is used. However, Mg- based sorbent seems to be less effective than the other two sorbents investigated. As shown in Figure 5a, magnesium vanadates are not present even at high temperatures. The reason is due to magnesium's high affinity to form magnesium sulfate even at high temperatures. Magnesium vanadate becomes dominant only when excess amount of sorbent is used as shown in Figure 6c.

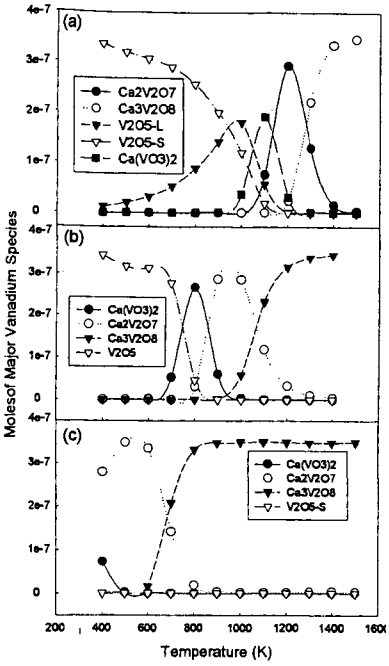


Figure 5 Impact of chlorine and sulfur on the effectiveness of Ca-based sorbent: a) typical concentration in coal; b) stoichiometric amount of sorbent to react with chlorine and sulfate; c) 20% excess of sorbent then the stoichiometric amount

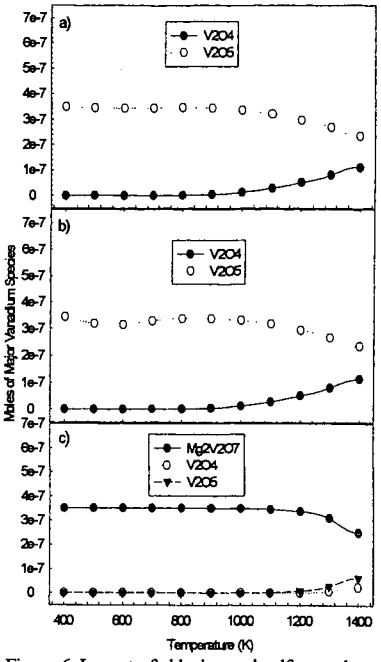


Figure 6 Impact of chlorine and sulfur on the effectiveness of Mg-based sorbent: a) typical concentration in coal; b) stoichiometric amount of sorbent to react with chlorine and sulfate; c) 20% 20% excess of sorbent then the stoichiometric amount

*Set IV : Determination of the most effective sorbent.*

To determine the most effective sorbent, in the final set of calculations all the sorbents were included. Calculations were first conducted for typical coal combustion assuming no chlorine or sulfur. Chlorine and sulfur concentrations in typical coal were then used. Finally, stoichiometric amounts of sorbent materials were used. The results are shown in Figures 7a-c, respectively.

Without chlorine or sulfur in the system, Na- based sorbent apparently is the most effective one in the entire temperature range investigated (Figure 7a). However, it has a stronger affinity to react with chlorine and sulfur. Hence, it becomes ineffective when chlorine or sulfur is present. On the other hand calcium is not significantly affected by the presence of chlorine. It is impaired by sulfur only at lower temperatures. Hence, Ca-based sorbent is more competent when chlorine or sulfur is present (Figure 7b). When stoichiometric amounts of sorbents are used, Ca- based sorbent is effective even at lower temperatures. This is probably due to the shielding effects of the presence of Na- and Mg- based sorbents as they are more vulnerable to chlorine and sulfur.

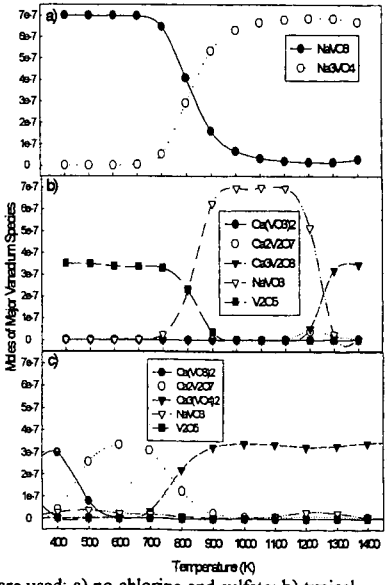


Figure 7 Partition of vanadium species when various amount of all sorbents are used: a) no chlorine and sulfate; b) typical coal combustion; c) stoichiometric amount of sorbents

## CONCLUSIONS

Vanadium is concentrated in various fuels and the emission of vanadium from combustion systems is of concern. Mineral sorbents have been demonstrated to be effective to control various toxic metals in combustion systems. In this study, equilibrium calculations were conducted to identify the potential sorbent materials to chemically adsorb vanadium. Na-, Ca- and Mg- based sorbents were found to be effective. However, the presence of chlorine and sulfur in the system may affect the performance of these sorbents. Na- based sorbent is significantly impaired when chlorine or sulfur is present. Sodium chloride and sulfate are formed under this condition. Ca- and Mg- based sorbents are less affected by chlorine but sulfur substantially reduces their performance. Sulfates are formed under this condition. The formation of sulfates or chlorides diminishes the available sorbents for vanadium capture. Calculations were also performed to determine the most effective sorbent. Na- based sorbent is found to be the most effective one when no chlorine or sulfur is present. However, Ca-based sorbent becomes the most robust one when chlorine or sulfur exists.

This study provides the insight of the reactions between vanadium and sorbents as well as the impact of various operating conditions. The information obtained can be used as a basis for developing a better strategy for managing vanadium emission problems.

## ACKNOWLEDGMENTS

The authors are grateful to the generous help from Dr. R. C. Reynolds, Department of Mechanical Engineering, Stanford University.

## REFERENCES

1. Yee, B. H.; Rosenquist, W. A., "Petroleum Coke as an Alternative Fuel for New Generation and Repowering"; Proc. Amer. Power Conf., **(2)**, 838-841, 1996. IL Inst. Tech., Chicago, IL.
2. Bryers, R. W., "Utilization of Petroleum Coke and Petroleum Coke/Coal Blends as a Means of Steam Raising", *Fuel Processing Technology*, v 44 n 1-3 Sep 1995., p 121-141
3. Lin, C.Y.; Chiu, C.H., "Emissions of Industrial Furnaces Burning Vanadium-Contained Heavy Oils", *J. Env. Sci. Health*, A: Env. Sci. Eng. & Toxic & Haz. Sub. Ctrl, **30(1)**, 1995,133-142.
4. Tsuboi; I. K., Kunugita, S., Komasawa, E., Isao Recovery of Gallium and Vanadium From Coal Fly Ash., *J Chem Eng* Jpn, **24(1)**, 1991, 15-20.
5. Biswas, P. and Wu, C. Y., "Control of Toxic Metal Emissions from Combustors Using Sorbents: A Review", *J. Air & Waste Management Association*, **48**, 1998, 113-127.
6. Scotto, M. V., Uberoi, M., Peterson, T. W., Shadman, F. and Wendt, J. O. L., Metal Capture by Sorbents in Combustion Processes, *Fuel Proc. Technol.*, **39(1/3)**, 1994, 357-372.
7. Wu, B., Jaanu, K. K. and Shadman, F., "Multi-functional Sorbents for the Removal of Sulfur and Metallic Contaminants from High-Temperature Gases", *Environ. Sci. Technol.*, **29(6)**, 1995, 1660-1665.
8. Venkatesh, S., Fournier, D. J. Jr., Waterland, L. R. and Carroll, G. J., "Evaluation of Mineral-Based Additives as Sorbents for Hazardous Trace Metal Capture and Immobilization in Incineration Processes", *Haz. Waste. Haz. Mat.*, **13(1)**, 1996, 73-94.
9. Owens, T. M. and Biswas, P., "Reactions between Vapor Phase Lead Compounds and *In Situ* Generated Silica Particles at Various Lead-Silicon Feed Ratios: Applications to Toxic Metal Capture in Combustors", *J. Air Waste Manage. Assoc.*, **46**, 1996, 530-538.
10. McMillin, B. K., Biswas, P. and Zachariah, M., "*In Situ* Diagnostics of Vapor Phase Growth of Iron Oxide-Silica Nanocomposites", Part I: 2-D Planar Laser-Induced Fluorescence and Mie Imaging, *J. Mater. Res.*, **11(6)**, 1996, 1552-1561.
11. Wu, C. Y., Lee, T. G., Arar, E., Tyree, G. and Biswas, P., "Capture of Mercury in Combustion Environments by *In-Situ* Generated Titania Particles with UV Radiation", *Env. Eng. Sci.*, **15(2)**, 1998, 137-148.
15. Owens, T., Wu, C. Y. and Biswas, P., "An Equilibrium Analysis for Reactions of Metal Compounds with Sorbents in High Temperature Systems", *Chem. Eng. Comm.*, **133**, 1995, 31-52.
17. Wu, C. Y. and Biswas, P., "An Equilibrium Analysis to Determine the Speciation of Metals in an Incinerator", *Combust. Flame*, **93**, 1993, 31-40.
12. Reynolds, W. C., "STANJAN-Interactive Computer Programs for Chemical Equilibrium Analysis", Dept. Mechanical Engineering, Stanford Univ., 1995.
13. Chase, M. W., Davies, C. A., Downey, J. R., Frurip, D. J., McDonald, R. A. and Syverud, A. N., JANAF Thermochemical Tables, 3rd Edition, *American Chemical Society and American Institute of Physics for the National Bureau of Standards*, Midland, MI, 1986.
14. Barin, I., "Thermochemical Data of Pure Substances", 3rd Ed., *VCH*, Germany, 1995.
16. Linak, W. P. and Wendt, J. O. L., "Toxic Metal Emissions from Incineration: Mechanisms and Control", *Prog. Energy Combust. Sci.*, **19**, 1993, 145-185.

# SUPERCRITICAL WATER GASIFICATION OF COAL USING CA(OH)$_2$ AS AN ADDITIVE

Jie Wang and Takayuki Takarada
(Department of Biological and Chemical Engineering,
Gunma University, Kiryu , Gunma 376, JAPAN)

**KEYWORDS:** supercritical water, coal gasification, calcium hydroxide

## ABSTRACT

A few coals were gasified under the supercritical water conditions in an autoclave at a temperature up to 700 °C and a pressure up to 30 Mpa. Calcium hydroxide was used both as a catalyst and an absorbent for the capture of $CO_2$. The carbon conversion, gas and liquid productions, $CO_2$ sorption by calcium and calcium utilization were determined in the experiments. Without the addition of Ca, the carbon conversion of Yallourn coal was about 44% at 690 °C and 28 Mpa; whereas the addition of Ca up to a Ca/C molar ratio of 0.6, the carbon conversion increased by 22%. Correspondingly, hydrogen yield was increased from 0.23 to 0.37 NL/g-coal (daf), methane yield from 0.16 to 0.19 NL/g-coal(daf), and ethane yield from 0.015 to 0.03 NL/g-coal(daf). At a Ca/C ratio of 0.6, almost no $CO_2$ remained in gas phase, with a calcium utilization value of 50-60%.

## INTRODUCTION

Gasification is one of the oldest coal utilization processes. The present paper is concerned with the gasification of coal in supercritical water at a temperature up to 700 °C and a pressure around 30 Mpa with the addition of calcium hydroxide. The essential idea concerning this research subject has been proposed by Lin et al [1]. They found that when several coals were gasified in supercritical water at temperatures 650-700 °C and a pressure of 60 Mpa using lime and a small amount of sodium compounds as additives, very high carbon conversion could be achieved with a high proportion of hydrogen and some $CH_4$ and CO in resultant gas. The following global reactions are principally taken into account in the gasification system:

$$C + H_2O \rightarrow CO + H_2 \qquad \Delta H_{900} = 140.3 \text{ kJ mol}^{-1} \qquad (1)$$

$$H_2O + CO \leftrightarrow CO_2 + H_2 \qquad \Delta H_{900} = -32.6 \text{ kJ mol}^{-1} \qquad (2)$$

$$Ca(OH)_2 \leftrightarrow CaO + H_2O \qquad \Delta H_{900} = 92.6 \text{ kJ mol}^{-1} \qquad (3)$$

$$CO_2 + Ca(OH)_2 \leftrightarrow CaCO_3 + H_2O \qquad \Delta H_{900} = -83.4 \text{ kJ mol}^{-1} \qquad (4)$$

$$CO_2 + CaO \leftrightarrow CaCO_3 \qquad \Delta H_{900} = -176.0 \text{ kJ mol}^{-1} \qquad (5)$$

Where the values of reaction heat change refers to those at a temperature of 900 K, a steam pressure of 30 Mpa and other gas pressures of 0.1 Mpa. As shown in reactions (4) and (5), lime or slaked lime can also play an important role in capturing environmentally unfriendly $CO_2$ and sulfur-bearing gases. As the released $CO_2$ gas is eliminated effectively by $Ca(OH)_2$ and/or CaO by reactions (4) and (5), CO can thus be highly transferred to hydrogen by enhancing the forward step of reaction (2).

In the present study, we aim at revealing catalytic effect of calcium hydroxide on supercritical water gasification of coal because no meticulous report has been documented regarding this interesting issue. We also would like to discuss the behaviors of calcium hydroxide for the retention of $CO_2$ in supercritical water.

## EXPERIMENTAL

Gasification was carried out in a 20 ml batch autoclave. In each run, a 0.2 g sample of coal mixed with the desired amount of $Ca(OH)_2$ was added into the reactor with the injection of around 3.5 ml distilled water. It typically took 20 min for temperature to rise from room temperature to 690 °C.

Compositional analysis of the resultant gas was carried on a gas chromatograph, which used molecular sieve column in one channel and HaySep A column in another with TCD detectors (detectable gasses: $H_2$, $O_2$, $N_2$, $CH_4$, CO, $CO_2$, $C_2$, $C_3$ and $C_4$). The reacted slurry was filtered to collect the liquid. Some of the filtrates were analyzed on a gas chromatograph to determine BTX, PCX and naphthalene. Effort was made to collect the solid with least loss. The solid was dried at 107 °C in flowing nitrogen and then subjected to the analysis of the forms of carbon in it (total carbon content and carbon content as $CaCO_3$) through a method of acid dissolution.

Reagent-grade calcium hydroxide was purchased from Wako Co. in Japan. Table 1 lists the characteristics of coal samples used in the study. The particle size of coal samples was screened between 60 and 100 Tyler mesh.

**Table 1.** Characteristics of Coal Samples used in the Study

| Coal sample | Proximate analysis (wt%, as-received) | | | | Ultimate analysis (wt%, daf) | | | | |
|---|---|---|---|---|---|---|---|---|---|
| | Moisture | VM | Ash | FC | C | H | N | S | O |
| Yallourn (YL) | 14.3 | 47.3 | 0.8 | 36.6 | 66.1 | 5.3 | 0.6 | 0.3 | 27.7 |
| Morwell (ML) | 10.0 | 46.3 | 1.4 | 43.3 | 67.9 | 5.0 | 0.5 | 0.3 | 26.3 |
| Tanitoharum (TN) | 4.6 | 48.8 | 5.0 | 41.6 | 76.3 | 5.6 | 1.4 | 0.2 | 16.5 |

## RESULTS AND DISCUSSION

Table 2 lists the yields of gases, carbon conversion and carbon recovery obtained at 690 °C and around 28 Mpa as functions of the Ca/C molar ratio. Runs 3 and 4 as well as runs 6 and 7 demonstrate the reproducibility of experiment. Carbon conversion refers to the sum of carbon fraction in gas phase and that in solid. No determination of liquid was considered in this series of experiment. Regardless of calcium addition, the main combustible gases produced were hydrogen and methane. With more calcium addition up to a Ca/C ratio of 0.6, an increase in the hydrogen yield concurrent with an increase in the carbon conversion was striking; whereas more $CO_2$ was fixed in the solid. At a Ca/C ratio of 0.6, virtually no $CO_2$ remained in the gas phase. In the presence of calcium, the yields of methane and ethane appeared to be somewhat larger than those in the absence of calcium. Antal and his collaborators ever made their efforts to produce a hydrogen-rich gas from biomass by supercritical water gasification at 600-650 °C and 30 Mpa [2]. In our study, it was shown that although the proportion of hydrogen in the resultant gas significantly increased, partly because of an increased carbon conversion to hydrogen via reactions (1) and (2), calcium hydroxide had no great effect on the decomposition of methane and ethane into hydrogen.

**Table 2.** Gas Yields and Carbon Conversion of YL coal with the Addition of $Ca(OH)_2$ (690±4 °C; 28±3 Mpa; holding time at the final temperature, 0 min)

| Run No. | Ca/C molar ratio (-) | Gas yield (NL/100g-coal daf) | | | | | $CO_2$ fixed (NL/100g-coal(daf) | Carbon conversion (%) | Carbon recovery (%) |
|---|---|---|---|---|---|---|---|---|---|
| | | $H_2$ | $CO_2$ | $CH_4$ | $C_2H_6$ | $C_3H_8$ | | | |
| 1 | 0 | 23.6 | 18.1 | 15.8 | 1.1 | nd | - | 43.9 | 86.5 |
| 2 | 0.15 | 24.0 | 8.3 | 15.8 | 2.2 | 0.02 | 16.4 | 52.1 | 87.5 |
| 3 | 0.30 | 29.0 | 2.4 | 15.7 | 2.4 | nd | 26.1 | 55.0 | 86.1 |
| 4 | 0.30 | 31.6 | 5.0 | 15.9 | 2.6 | nd | 27.7 | 60.8 | 84.6 |
| 5 | 0.45 | 35.5 | 0.8 | 16.6 | 2.1 | nd | 30.6 | 64.4 | 79.6 |
| 6 | 0.60 | 38.9 | 0.1 | 19.2 | 2.6 | nd | 37.0 | 69.4 | 82.1 |
| 7 | 0.60 | 35.4 | 0.02 | 18.5 | 3.2 | 0.03 | 40.1 | 67.6 | 86.8 |

nd, not detected (the same as below)

Because the carbon conversion was not as high as expected even with twice amount of $Ca(OH)_2$ added to coal, the reaction was prolonged to examine the gasification of remaining char and the results are listed in Table 3. Surprisingly, in the absence of catalyst, an increase in the carbon conversion was so slight even for prolonging the reaction for 20 min. At a Ca/C ratio of 0.6, hydrogen yield to some degree increased, with the increase of carbon conversion. From these data, we can see that the gasification of residual char was slow even under the supercritical water conditions and with the addition of calcium. We noticed that the molar ratio of $H_2$ to $CO_2$ was around 1, half lower than the stoichiometric ratio by reactions (1) and (2). This may be because some hydrogen can be consumed in the formation of $CH_4$, and also because part of $CO_2$ can be derived from the volatile of coal.

Table 4 shows the results of the gasification of MW coal and TN coal. It was observed that calcium hydroxide also had an effect on enhancing gasification of these two coals to produce more hydrogen. The three coals used in the study were all young coals which may be better suitable for the gasification in supercritical water. When higher-rank bituminous coals were gasified (not shown here), the carbon and hydrogen yields were relatively low as compared with those obtained for these three coals.

**Table 3.** Gas Yields and Carbon Conversion of YL Coal Gasified for Different Holding Times at Final Temperature (680±4 °C; 30±2 Mpa).

| Run No. | Ca/C molar ratio | Holding time (min) | Gas yeild (NL/100-coal(daf) | | | | | $CO_2$ fixed (NL/100g-coal(daf) | Carbon conversion (%) | Carbon recovery (%) |
|---|---|---|---|---|---|---|---|---|---|---|
| | | | $H_2$ | $CO_2$ | $CH_4$ | $C_2H_6$ | $C_3H_8$ | | | |
| 8 | 0 | 0 | 25.8 | 18.0 | 15.7 | 1.4 | nd | - | 44.7 | 86.3 |
| 9 | 0 | 10 | 32.3 | 20.7 | 14.8 | 1.4 | nd | - | 47.2 | 85.8 |
| 10 | 0 | 20 | 36.8 | 18.9 | 17.6 | 1.3 | 0.02 | - | 46.0 | 86.7 |
| 11 | 0.3 | 0 | 25.5 | 0.8 | 15.4 | 2.4 | nd | 30.4 | 59.4 | 83.4 |
| 12 | 0.3 | 10 | 40.4 | 6.6 | 21.1 | 3.2 | nd | 27.8 | 69.6 | 82.1 |
| 13 | 0.6 | 10 | 43.4 | 0.3 | 20.9 | 2.9 | 0.06 | 43.8 | 71.7 | 87.7 |
| 14 | 0.6 | 20 | 46.9 | 1.8 | 23.5 | 2.9 | 0.02 | 42.3 | 74.8 | 86.5 |

**Table 4.** Gas Yields and Carbon Conversion in the gasification of MW coal and TN coal (688 ±2 °C; 28 ±2 °C; holding time, 0 min)

| Run No. | Coal sample | Ca/C molar ratio | Gas yield (NL/100-coal(daf) | | | | | $CO_2$ fixed (NL/100g-coal(daf) | Carbon conversion (%) | Carbon recovery (%) |
|---|---|---|---|---|---|---|---|---|---|---|
| | | | $H_2$ | $CO_2$ | $CH_4$ | $C_2H_6$ | $C_3H_8$ | | | |
| 15 | MW | 0 | 23.2 | 17.1 | 13.3 | 1.7 | 0.004 | - | 47.4 | 79.8 |
| 16 | MW | 0.45 | 38.3 | 0.03 | 17.5 | 2.3 | 0.08 | 39.7 | 61.2 | 87.4 |
| 17 | TT | 0 | 21.4 | 14.2 | 14.5 | 2.4 | 0.004 | - | 49.7 | 74.7 |
| 18 | TT | 0.45 | 35.6 | 0.01 | 14.1 | 2.5 | 0.3 | 31.2 | 59.6 | 79.4 |

We noticed that the values of carbon recovery shown in Tables 2-4 were not beyond 90%. Despite a small part of carbon loss which was unavoidable in the experimental procedures, the deficient amount of carbon recovery lower than 100% might be mainly due to the excluded carbon fraction in tarry materials. However, some of the filtrates were determined in the amounts of light hydrocarbons, and the partial analysis data and the values of carbon closure through the analysis of light hydrocarbons are given in Table 5. We found that at lower temperatures, the values of carbon closure were still significantly lower than 100% but the balance was enhanced at higher temperatures. At lower temperatures, there obviously existed more BTX, PCX, with more tar that was not determined. In the visible observation, the water solutions separated after filtration were brown in color while the solution obtained at higher temperatures were essentially transparent. An important observation was that calcium oxide had a marked effect on the decomposition of coal in supercritical water. More tarry materials may be formed via promoting hydrolysis and dissolution into dense supercritical water, as well as via preventing the secondary reaction from depolymerization, under the effects of $Ca(OH)_2$ in supercritical water.

**Table 5.** Carbon Partition into gaseous, liquid and solid products for YL coal.

| Experimental conditions | | | | Carbon partition (% of total carbon) | | | | | | | | Carbon closure (%) |
|---|---|---|---|---|---|---|---|---|---|---|---|---|
| FT (°C) | Ca/C (-) | HT (min) | P (Mpa) | gaseous $CH_4$ | gaseous $CO_2$ | gaseous $C_2$ | gaseous $C_3$ | BTX | PCX | $C_6H_6$ | solid * | |
| 568 | 0 | 13 | 24 | 3.3 | 5.4 | 0.5 | 0.1 | 1.0 | 1.0 | 0.1 | 60.9 | 72.3 |
| 565 | 0.3 | 13 | 25 | 3.1 | 0.0 | 1.2 | nd | 0.4 | 1.2 | 0.2 | 67.2 | 74.6 |
| 560 | 0.60 | 12 | 28 | 4.2 | 0.0 | 1.5 | 0.4 | 0.4 | 1.6 | 0.0 | 68.3 | 76.3 |
| 680 | 0 | 20 | 32 | 12.6 | 14.7 | 2.3 | 0.1 | 0.0 | 0.7 | 0.0 | 57.8 | 88.3 |
| 683 | 0.6 | 20 | 29 | 17.0 | 0.1 | 4.7 | 0.1 | 0.0 | 0.6 | 0.0 | 63.2 | 88.0 |

*, including carbon as $CaCO_3$ and organic carbon

Figure 1 displays the relation of $CO_2$ sorption and calcium utilization with Ca/C molar ratio. In the case of almost complete retention of $CO_2$, the value of calcium utilization was 50-60%. When prolonging the reaction, carbon dioxide was not effectively captured by remaining calcium, as illustrated in Figure 2. However, it remained doubtful how much the $CO_2$ could possibly be captured during cooling stage.

## ACKNOWLEDGMENTS

We thank Drs. Lin S. Y., Hatano H. and Suzuki Y. at National Institute for Resource and Environment for their discussion and assistance in this subject of research. The financial support from CCUJ, Japan is greatly appreciated.

## REFERENCES


1. Lin S. Y., Suzuki Y. and Hatano, H., Harada, M. A New Method (Hypr-RING) for Producing Hydrogen from Coal. In Prospects for Coal Science in the 21st Century (editors, Li B. Q and Liu Z. Y.). 1999. Shanxi Sic. Tech. Press: 475-478.

2. Xu X.and Antal M. J. Environmental Progress. 1998, 17, 215.


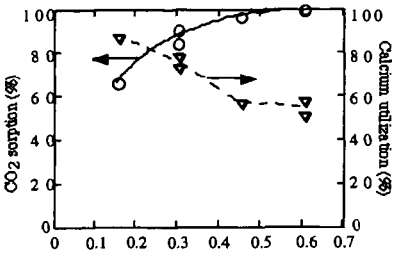


**Figure 1.** $CO_2$ sorption and calcium utilization the amount of $Ca(OH)_2$ added (690 °C, 28 Mpa, 0 min holding time).

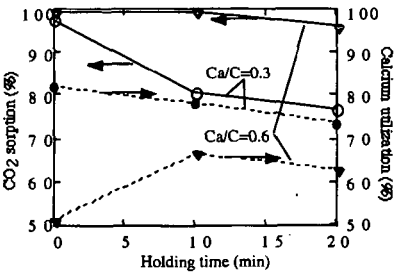


**Figure 2.** $CO_2$ sorption and calcium utilization with holding time at varying Ca/C molar ratio (680 °C, 30 Mpa).

# THE IMPACT OF CHLORINE ON HEXAVALENT CHROMIUM EMISSIONS FROM A LAMINAR DIFFUSION FLAME

**Bing Guo and Ian M. Kennedy**
**Department of Mechanical and Aeronautical Engineering**
**University of California**
**Davis, CA 95616**
**USA**

ABSTRACT

Measurements of total chromium and hexavalent chromium have been obtained in a laminar hydrocarbon/air diffusion flame. Chlorine was added to the fuel as methyl chloride gas. A probe sampled the emissions from the flame. Particles were collected on a filter and vapor phase species were collected in impingers. Hexavalent chromium was measured with a spectrophotometric method. Total chromium added to the flame was determined by gravimetric analysis of the chromium source, chromium hexacarbonyl. The fraction of hexavalent chromium increased significantly as small amounts of chlorine were added. Partitioning between phases was also altered – much more hexavalent chromium was found in the impingers as the chlorine loading increased. Differential mobility analysis of the particles showed that the mean particle size was always in the range of 25-30 nm, whether chlorine was added or not. However, particle concentrations decreased when chlorine was present. Equilibrium calculations showed strong sensitivity to the thermochemical properties of the included species, particularly $CrO_2Cl_2$.

KEYWORDS: hexavalent chromium, chlorine, laminar diffusion flame

## INTRODUCTION

Metals are often unavoidably introduced into combustion systems. Coal combustion ineluctably introduces metals as part of the mineral matter of the fuel. The incineration of many wastes also suffers a similar problem. Many of these metals can exist in more than one oxidation state, some are of great environmental concern. It is known that the toxicity of the metals is a strong function of the oxidation state. For example, the hexavalent form of chromium is much more toxic than the trivalent form [1, 2]. The physical state of the metal may also depend upon its chemical state, with significant implications for the selection of air pollution control equipment.

The problem of metal transformation and fate is exacerbated in waste incineration when chlorine is present. Many waste streams introduce chlorine as part of the waste itself. The presence of chlorine in the mixture will result in an increase in the emission of vapor phase metals, as the metal chlorides are generally more volatile than the metal oxides. Furthermore, Linak and Wendt [3] showed, via equilibrium calculations, that chlorine has a significant impact on the fraction of the total chromium that appears as hexavalent chromium, primarily through the enhanced formation of the hexavalent $CrO_2Cl_2$ at a temperature around 700K. This temperature is expected in the post flame gases, and gives rise to the possibility that hexavalent chromium may be formed in the downstream sections of an incinerator if sufficient residence time is available.

A number of earlier studies of the fate of metals in combustion systems have focused on simulations of realistic incinerator conditions [3-5]. Fewer studies have been undertaken in simple flame configurations that are amenable to theoretical or numerical modeling. Premixed flame studies, such as that of Bulewicz and Padley [6], are useful in gaining an understanding of the kinetics of metal oxidation. However, practical combustion systems generally utilize non-premixed reaction. Yoon et al. [7] studied a laminar, hydrogen/air diffusion flame that was seeded with chromium and found that high temperatures favored the formation of hexavalent chromium. They did not add chlorine to the flame.

This paper is an extension of the earlier work of Yoon et al. [7]. It considers the impact of chlorine in a laminar hydrocarbon/air diffusion flame, with particular attention to the issues of speciation of chromium and partitioning between solid and vapor phases. The measurements and equilibrium analysis reveal the impact of varying temperature and oxygen concentration on chromium speciation in the presence of chlorine.

## EXPERIMENTAL

The coflow, laminar, diffusion flame system is shown in Fig. 1. The 5 mm burner nozzle was positioned in the center of a 100×100 mm duct containing flow straighteners and a series of fine-mesh screens to ensure air-flow uniformity. Methane ($CH_4$) was used as the primary fuel in this experiment. A small quantity of $CH_3Cl$ was added into the fuel as a chlorine source. The flow rate of $CH_4$ was adjusted, according to the $CH_3Cl$ flow rate, so as to keep the mixture flow rate constant. The mole fraction of $CH_3Cl$ in the fuel was in the range from zero to 0.07.

Chromium hexacarbonyl ($Cr(CO)_6$), a volatile crystal that decomposes at 210 °C to produce elemental Cr, was used as a chromium source in the experiment. A glass cartridge containing chromium hexacarbonyl was added to the fuel delivery line. The $CH_4/CH_3Cl$ mixture flowed through the cartridge at a rate of 0.160 L/min. With temperature controlled at 24 °C, the vapor pressure resulted in a chromium concentration of 60 ppmv. The concentration of chromium in the carrier gas was obtained gravimetrically by comparing the mass difference of chromium hexacarbonyl in the cartridge before and after the experiment. Chromium hexacarbonyl vapor carried in the fuel decomposed quickly in the flame to provide zero-valence chromium.

Samples of vapor and particle phases of chromium compounds emitted from the flame were obtained with a stainless steel sampling probe positioned above the flame on the centerline. The 200-mm-long, 22-mm-outer diameter sampling probe contained a 150-mm-long, 13-mm-inner diameter sintered metal tube as its inner wall. Nitrogen dilution gas was provided to the sampling probe through its inner wall and mixed with the sample to quench reactions, the development of aerosols through the sampling lines, and to minimize the transport of particles and vapors to the probe wall. The flow rate of nitrogen was fixed at 0.8 L/min, accounting for more than 25% of the total sampling flow rate, which was deemed adequate to serve those purposes mentioned above [7].

Figure 2 shows the chromium sampling system. The particle phase of chromium, and some absorbed gas phase material, was captured on a 47-mm-diameter alumina membrane filter with 20 nm pores. The temperature of the filter, and the sampling lines between the probe and the filter, was kept slightly above 100°C by heating with heating tapes, to prevent water condensation along the lines and on the filter, and avoid interconversion between Cr(VI) and Cr(III). All of the samples were obtained above the flame tip at a distance of 55 mm from the nozzle exit where the temperature was 1400 °K on the centerline. The flame tip was approximately 26 mm from the nozzle exit for all the experiments.

The impingers and liquid nitrogen trap were designed to capture the vapor phase of the chromium compounds. A $NaHCO_3$ solution was used in the impingers to prevent further conversion between Cr(VI) and Cr(III). HCl was a major product of the $CH_4/CH_3Cl$ flame; the pH of the $NaHCO_3$ buffer solution was adjusted to accommodate the $CH_3Cl$ concentration in the fuel and the resultant concentration of HCl in the sample.

The sampling time for each sample was 1 hour. The filter was cut into two halves, one for hexavalent chromium analysis and another for total chromium analysis. Samples from the impingers and the liquid nitrogen trap were analyzed solely for hexavalent chromium. Sampling lines before the filter were rinsed with deionized water for hexavalent chromium analysis. In the experiments reported herein, there was no measurable amount of hexavalent chromium detected in the samples from the liquid nitrogen trap and those from rinsing the sample lines.

The half filter for Cr(VI) analysis was extracted with a 0.01 N $NaHCO_3$ solution for 20 hours before the extraction solution was analyzed by a spectrophotometric method as described in EPA Method 7196A [8]. An X-ray fluorescence (XRF) method was used to measure the total chromium on the filter with a Kevex 0700/8000 energy dispersive XRF spectrometer. Total chromium consumed in the experiment was determined from the mass difference of the chromium hexacarbonyl in the cartridge before and after the experiment with a Mettler AJ100 balance.

A TSI Model 3934 SMPS (Scanning Mobility Particle Sizer) system was used for the particle size analysis. A denuder containing sodium hydroxide was added to the sampling line to eliminate $H_2O$ and HCl from the sampled post flame gases. A post flame aerosol stream of 0.6 L/min was fed into the particle size analyzer.

## RESULUTS AND DISCUSSION

A series of samples were taken at a fixed sampling point 55 mm above the nozzle to study the combustion products with varying chlorine concentrations in the fuel. With the chlorine concentrations that were used in these experiments, the flame length did not show a measurable change. Cr(VI) mass on the filter was compared with the total chromium mass on the filter. As an abbreviation, this fraction is referred to as "on-filter Cr(VI) fraction" hereafter. The total Cr(VI) mass from both the filter and the impingers was compared with the total chromium consumed in the experiment, and this fraction is referred to as "overall Cr(VI) fraction" hereafter. The Cr(VI) emitted in the vapor phase and trapped in the impingers was compared with the total chromium consumed in the experiment. This fraction is referred to as "gas-phase Cr(VI) fraction" later in this paper. Similarly, the Cr(VI) captured on the filter was compared with the total chromium consumed in the experiment, and this fraction was referred to as "solid-phase Cr(VI) fraction" hereafter. The fraction of the total input chromium that was recovered was evaluated by comparing chromium recovered on the filter and in the impingers with the total chromium supplied in the fuel. Without chlorine we found typical recoveries of input chromium

of about 10%. As chlorine was added, the recovery rate increased to up to 64%, as a result of a greater amount of Cr(VI) passing through the filter to the impingers and being detected by the spectrophotometric method.

Figure 3 shows the overall Cr(VI) fraction of the total chromium added to the flame; it is plotted against varying $CH_3Cl$ concentrations in the fuel. Since it was possible that some of the flame emission was not collected into the sampling probe, this fraction can be interpreted as a lower limit of the Cr(VI) fraction. Nevertheless, the samples showed a clear increase in Cr(VI) with increasing $CH_3Cl$ concentration in the fuel. This trend is consistent with measurements in practical systems. Volland [9] reported results from a variety of tests on medical waste incinerators in which stainless steel "sharps" may provide a significant source of chromium. Without chlorine in the feed, about 16% of the stack gas chromium appeared in its hexavalent state. With 8.5% chlorine in the feed, the fraction of hexavalent chromium increased to about 48%. Our results confirm the strong impact of chlorine on the propensity to form hexavalent chromium.

It was also found that the on-filter Cr(VI) fraction increased to 1 as only a small amount of chlorine was added, while the typical value for samples from experiments without chlorine was around 0.2, as illustrated in Figure 4. The increase in the on-filter hexavalent fraction was accompanied by a change in the color of the filter. Without chlorine, the filters were reddish-brown, suggestive of $CrO_3$. As chlorine was added, the filters changed color to green and further yielded a light green solution when extracted with water. We expect, from equilibrium calculations discussed later, and from its solubility, that the compound $CrO_2Cl_2$ may be responsible for the observed color change.

The presence of chlorine affects not only the chemical state of the metal, but also its physical state, largely as a result of the formation of more volatile metal chlorides that tend to yield gas phase products. Sampling at the same point above the flame showed that gas-phase Cr(VI) increased with increasing concentration of chlorine in the fuel, while the solid-phase Cr(VI) fraction remained at a steady level for all the chlorine concentrations, as shown in Figure 5. This trend is in agreement with observations from practical incinerators [9].

Differential mobility particle analysis showed some impact of chlorine on the particle size distribution in the post flame gases. While the mean particle size was always found to be in the range of 25-30 nm, not very sensitive to $CH_3Cl$ concentration in the fuel, a decrease by a factor of 10 was observed in particle concentration when $CH_3Cl$ concentration in the fuel increased to about 0.03. This is in agreement with the increase in gas-phase Cr(VI) associated with increasing $CH_3Cl$ concentration in the fuel.

An equilibrium calculation considered the following species: $CH_3Cl$, $CH_4$, CO, $CO_2$, $Cl_2$, Cr, $CrOCl_2$, $CrOH_3$, CrOOH, $CrO_2$, $CrO_2Cl$, $CrO_2OH$, $CrO_2(OH)_2$, $CrO_3$, $Cr_2O_{3(s)}$, HCl, $H_2O$, $N_2$, and $O_2$. This list is by no means an exhaustive compilation of all possible species. As Linak and Wendt [3] and Kashireninov and Fontijn [10] pointed out, equilibrium calculations can be affected dramatically by the choice of species that are included. Nevertheless, the important species that were identified by these authors were included in the calculation. In addition to the impact of the choice of species, we have found that uncertainties in the thermochemical data, in particular that for the species $CrO_2Cl_2$, can be important. The enthalpy of formation for $CrO_2Cl_2$ reported by Ebbinghaus [12] was -519.2 kJ/mol, slightly higher than that reported by Barin [11] of -538.062 kJ/mol. Calculation showed that with these different values of enthalpy of formation, the equilibrium concentration of $CrO_2Cl_2$ could vary by a factor of 10. We have chosen to use the heat of formation for $CrO_2Cl_2$ that was reported by Barin. The results of a STANJAN calculation are presented in Fig. 6 in which $Cr_2O_3$ was considered to be in its solid form. The temperature was found from imposing an adiabatic condition.

The predicted equilibrium fraction of hexavalent chromium exhibits a maximum at a temperature of about 1400 °K. In contrast, Kashireninov and Fontijn [10] found a maximum in the Cr(VI) fraction at a temperature of about 1600 °K. Furthermore, these authors found that $CrO_2Cl_2$ was not significant down to temperatures of 1000 °K. Wu and Biswas [13] reported equilibrium results for the $CH_4$-air-$Cl_2$ system at temperatures of 1100 °K and 1500 °K. They used a combination of data from Barin [11] and Ebbinghaus [12]. The equilibrium results showed that $CrO_2Cl_2$ was not significant until temperatures dropped below 1000 °K. At higher temperatures, $CrO_2(OH)_2$ was the dominant hexavalent species. On the other hand, Linak and Wendt [3] showed that $CrO_2Cl_2$ was an important species in equilibrium over a broad range of temperatures from 500 °K to 1500 °K. The importance of $CrO_2Cl_2$ is apparent in Fig. 6. It is the dominant hexavalent chromium species in very lean mixtures and, of course, only appears when chlorine is present. In richer mixtures at concomitantly higher temperatures, chlorine makes little difference in the equilibrium fraction of hexavalent chromium.

The relevance of the equilibrium predictions to the measurement that we have undertaken can be understood if the equilibrium concentrations are plotted as a function of temperature and equivalence ratio. The equivalence ratio was obtained from thermocouple temperature

measurements. It was assumed that heat-releasing chemical reactions were complete at the measurement locations in the post flame gases. An adiabatic mixing calculation was performed to find the number of moles of air that were required to mix with combustion products to achieve the measured temperature. Equilibrium calculations were then run for the measured temperature and estimated equivalence ratio as a function of radial location. The temperature profile and the equilibrium mole fractions are shown in Fig. 7. It should be recalled that the sampling probe drew in most of the post flame gases. The measured hexavalent chromium fraction on the filter and in the impingers arises from streamlines that have passed through both the centerline of the flow and through peripheral regions. Temperatures and equivalence ratios in the latter regions are lower than along the centerline. The increase in Cr(VI) with chlorine addition can be understood in terms of an increase in $CrO_2Cl_2$ at the cooler edges of the flow. Equilibrium calculations suggest that Cl addition should have little impact on Cr speciation in the hotter gases on the centerline of the flow. The change in color of the filter with chlorine addition is consistent with this structure of the flow.

## CONCLUSIONS

Chromium sampling in a $CH_4/CH_3Cl$ flame has been performed using an $N_2$ dilution sampling probe, an alumina membrane filter, two impingers and a liquid nitrogen trap. All the samples were analyzed by EPA Method 7196A and X-ray fluorescence spectrometry to quantify the amounts of Cr(VI), and the partitioning of Cr(VI) phases. Flame products were analyzed with a TSI Model 3934 SMPS particle size analyzer. The results of Cr sample analysis showed a significant Cr(VI) fraction increase in the post flame gases with increasing concentration of $CH_3Cl$ in the fuel. The fraction of Cr(VI) emitted as vapor increased with increasing $CH_3Cl$ concentration in the fuel. It was also found that the color of the sample on the filter changed from dark brown to light yellow-green as $CH_3Cl$ concentration in the fuel increased, which suggested there was a change in the species distribution among the combustion products. This change was attributed to the increased presence of $CrO_2Cl_2$ in the post flame gases. Particle size analysis showed that the particle concentration in post flame gases decreased with increasing $CH_3Cl$ concentration in the fuel, while no significant change was found in the mean particle diameter as $CH_3Cl$ concentration in the fuel varied. Equilibrium calculations agreed with the observed Cr(VI) fraction change with varying $CH_3Cl$ concentration if the enhanced Cr(VI) yield is ascribed to enhanced $CrO_2Cl_2$ formation on the edge of the jet. The equilibrium results showed some sensitivity to the choice of thermochemical properties of $CrO_2Cl_2$.

## ACKNOWLEDGEMENTS

This research has been supported by the Superfund Basic Research Program with Grant 2P42ES04699-14 from the National Institute of Environmental Health Sciences, NIH with funding provided by EPA. Its contents are solely the responsibility of the authors and do not necessarily represent the official views of the NIEHS, NIH or EPA.

## REFERENCES

1. Flora, S. D. and Wetterhahn, K. E.: *Life Chem. Reports* 7, 169 - 244 (1989).

2. Flora, S. D., Bagnasco, M., Serra, D. and Zanacchi, P.: *Mutation Research* 238, 99 - 172 (1990).

3. Linak, W. P. and Wendt, J. O. L.: *Prog. Energy Combust. Sci.* 19, 145 - 185 (1993).

4. Fournier, D. J., W.E. Whitworth, J., Lee, J. W. and Waterland, L. R.: *The Fate of Trace Metals in a Rotary Kiln Incinerator with a Venturi/Packed Column Scrubber*, EPA/600/S2-90/043 EPA, 1991.

5. Linak, W. P., Srivastava, R. K. and Wendt, J. O. L.: *Combust. Sci. Tech.* 101, 7 - 27 (1994).

6. Bulewicz, E. M. and Padley, P. J.: *Proc. Roy. Soc. Lond. A.* 323, 377 - 400 (1971).

7. Yoon, Y., Reyes, C., Jones, A. D., Kelly, P., Chang, D. P. Y. and Kennedy, I. M.: *TwentySixth Symposium (Int.) on Combustion*, p. 1953 - 1959, The Combustion Institute, Pittsburgh,1996.

8. *Test methods for evaluating solid waste: physical/chemical methods*, U.S. EPA, Office of Solid Waste and Emergency Response, 1986.

9. Volland, C. S.: *85th Annual Meeting AWMA*, Paper 92-40.1, 1992.

10. Kashireninov, O. E. and Fontijn, A.: *Combust. Flame* 113, 498-506 (1998).

11. Barin, I.: *Thermochemical Data of Pure Substances*, VCH, Weinheim, Germany, 1993.

12. Ebbinghaus, B. B.: *Combust. Flame* 93, 119 - 137 (1993).

13. Wu, C. Y. and Biswas, P.: *Combust. Flame* 93, 31 - 40 (1993).

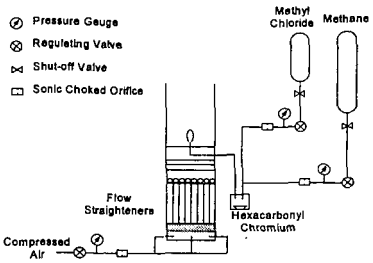


Figure 1 Schemetic of experimental apparatus

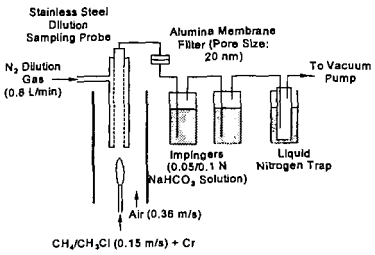


Figure 2 Schematic of chromium sampling system

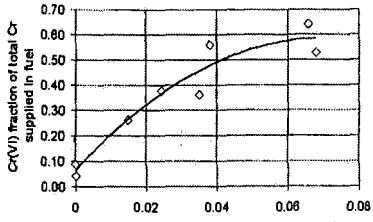


Figure 3 Cr(VI) Fraction of Total Cr Supplied in Fuel vs. CH3Cl Concentration in Fuel

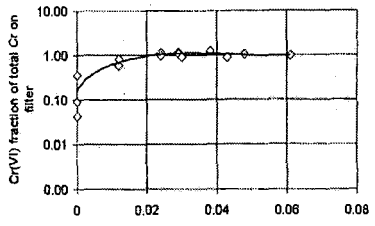


Figure 4 Cr(VI) Fraction of Total Cr on Filter vs. CH3Cl Concentration in Fuel

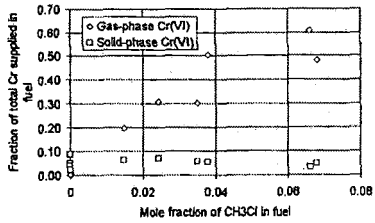


Figure 5 Gas-phase and Solid-phase Cr(VI) Fraction of Total Cr Supplied in Fuel vs. CH3Cl Concentration in Fuel

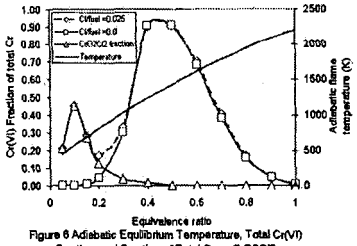


Figure 6 Adiabatic Equilibrium Temperature, Total Cr(VI) Fraction, and Fraction of Total Cr as CrO2Cl2

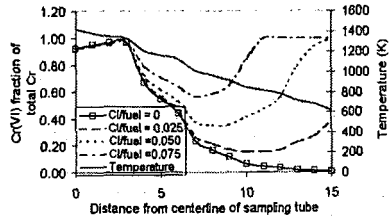


Figure 7 Measured Temperature Profile across Flame at Sampling Location and Calculated Equilibrium Cr(VI) Fraction of Total Cr

# CONTROL OF HEAVY METAL EMISSIONS FROM INCINERATION OF CCA-TREATED WOODS

Chang-Yu Wu, Kenjiro Iida, John Pierman, Thabet Tolaymat and Timothy Townsend,
University of Florida, Dept. Environmental Engineering Sciences, Gainesville, FL 32611-6450

**Key Words:** CCA wood, leaching, emission.

## INTRODUCTION

Chromium Copper Arsenate (CCA) has been used as a wood preservative since the 1970s. The production of CCA-treated woods has increased approximately 12 fold from 1970 to 1996.[1] By 1996, 79% of all the treated wood produced in the US, approximately 13 million cubic meters, was CCA-treated wood. Within Florida, 1 million pounds of the chemical were disposed during 1996.[2] Solo and Townsend[1] reported that by 2016 it would reach 6.8 million pounds. In Florida, the majority of the CCA-treated waste is processed through construction and demolition recycling facilities, resulting in a wood waste composition containing on average 6% CCA-treated wood. The primary market for wood waste is energy recovery and, therefore the majority of CCA-treated wood waste is burned for energy recovery purposes.[1]

During combustion, the heavy metals in these woods may escape from the combustion system and can be emitted into the atmosphere. Arsenic is known to be a volatile metal and is likely to enter the gas stream by vaporization.[3] Hirata *et al.*[4] performed an isothermal pyrolysis of CCA-treated wood and reported that almost all chromium and copper from the CCA woods were recovered from the ash while the majority of arsenic evolved into the gas phase. Once the metallic vapors exit the high temperature region and enter the low temperature region downstream, they may form submicrometer-sized aerosols.[5] Unfortunately, conventional air pollution control devices such as electrostatic precipitators (ESPs) have their minimum collection efficiencies at the submicrometer range.[6-8]

After combustion, the heavy metals are concentrated in the remaining ash[1]. The concentration of arsenic, chromium, and copper in the ash ranged from 8980~45000 mg/kg, 1780~22500 mg/kg, and 2720~31500 mg/kg, respectively.[1] Pohlandt *et al.*[9] conducted distilled water extraction on furnace, boiler, and fly ash produced from the combustion of CCA-treated wood. They reported that furnace ash produced the highest chromium concentrations (greater than 1,000 mg/L) and the fly ash produced the highest arsenic concentrations. Messick *et al.*[10] performed TCLP and SPLP on the ash obtained from the combustion of various retention levels of CCA-treated wood. The TCLP limits were exceeded for arsenic in almost all of their CCA ash samples. Half of their CCA ash results exceeded the TCLP limit for chromium. Once a waste is regulated as hazardous it must be disposed differently from regular wastes, which eventually increases the cost, the paperwork, and the labor needed for their disposal.

To prevent these undesirable consequences, a new technique needs to be developed. Using mineral sorbent materials to control heavy metals has been studied by a number of researchers since the late 1980s.[3, 11-13] Uberoi and Shadman[11] and Ho *et al.*[12] used silica, alumina and various naturally available materials (*i.e.*, bauxite, kaolinite and lime) to capture lead and cadmium. Mahuli *et al.*[3] demonstrated that calcium hydroxide can effectively capture volatile gaseous arsenic and confirmed the presence of calcium arsenate in the ash. Gullett and Ragnunathan[13] observed the reduction in submicrometer concentrations of arsenic when hydrated lime and limestone were injected into the combustion system. Chen and Wey[14] studied the effects of various operating conditions, such as the presence of organic chloride (PVC), inorganic chloride (NaCl), and sodium sulfide ($Na_2S$), on the capacity of a sorbent (limestone) to capture the heavy metals during combustion. The experiences of these researchers suggest that sorbent technology can be applied to the incineration of CCA-treated wood. The common mineral sorbents will potentially react with the heavy metals within the CCA-treated wood and also may impact the leaching behavior of these metals.

The objective of this research is to control both the emissions and leaching of heavy metals from the incineration of CCA-treated woods by using sorbent materials. Equilibrium calculations were performed to identify potential materials that can effectively bind those metals. Experiments were conducted to study their performance. The information obtained in this study will result in a better management option for CCA-treated wood disposal.

## EQUILIBRIUM MODELING

In a high temperature system, reactions are generally very fast, and equilibrium conditions are possibly achieved. Hence, thermodynamic equilibrium calculations can be used to predict the behavior of a high temperature system. In this study, thermodynamic equilibrium calculations were performed to identify the sorbent materials which can potentially react with the heavy metals in the CCA-treated wood. The effects of sulfur and chlorine, on the formation of sorbent-metal compounds were also analyzed. Available thermochemical data were gathered[15, 16] and the data of any relevant reactants and possible products were included in the calculations. The calculations were performed using the software STANJAN.[17] The calculations were performed assuming 100% excess air for a wide temperature range. The simulation conditions are listed in Table 1.

Table 1. Simulation conditions in each calculation.

| Calculation # or Figure # | Type of Sorbent Tested | Moles of Species Included in Calculation | | | | | |
|---|---|---|---|---|---|---|---|
| | | Sorbent | | | | | |
| | | Metal | $NaHCO_3$ | KOH | MgO | S | Cl |
| 1 | Na | 1 | 2 | N/A | N/A | 0 | 0 |
| 2 | | 1 | 2 | N/A | N/A | 0 | 10 |
| 3 | | 1 | 2 | N/A | N/A | 10 | 0 |
| 4 | Mg | 1 | N/A | N/A | 0.5 | 0 | 0 |
| 5 | | 1 | N/A | N/A | 0.5 | 0 | 10 |
| 6 | | 1 | N/A | N/A | 0.5 | 10 | 0 |
| 7 | Na, Mg, K | 1 | 2 | 2 | 0.5 | 0 | 0 |
| 8 | | 1 | 2 | 2 | 0.5 | 10 | 10 |

Chromium-Sorbent System

Calculations were first performed for chromium. Figure 1 shows the result of using a Na-based sorbent. As shown, sodium chromate ($Na_2CrO_4$) is the thermodynamically most stable compound among other possible chromium compounds. The result indicates the potential use of Na-based sorbents. Chlorine and sulfur are known to have strong affinity to react with many metals and hence their impact on the sorbent's performance is investigated. As shown in Figure 2, when chlorine is present in the system, chlorine consumes all the sodium available for chromium and forms sodium chloride (NaCl) at temperatures below 500°C and above 1200°C. Between 500°C and 1200°C, hydrochloric acid is more thermodynamically stable than NaCl; therefore, Na becomes available for chromium to form $Na_2CrO_4$. Thus, the Na-base sorbent is effective only at that temperature range. Figure 3 shows the effect of sulfur. As shown, when sulfur is present in the system, chromium sulfate is the major chromium species up to around 550 °C. Above this temperature, $Cr_2O_3$ becomes the dominant chromium species. Sodium is in the form of $Na_2SO_4$ only above 1000°C when the sodium sorbent becomes effective.

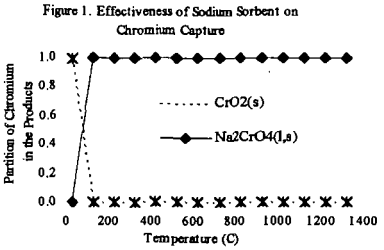


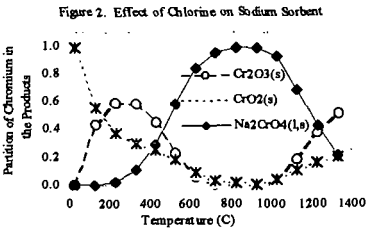


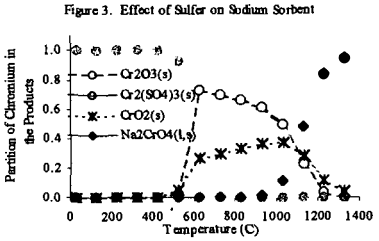


Calculations were also performed for the alkaline earth metal-based sorbents. The result for a Mg-based sorbent is shown in Figure 4. As shown, magnesium can also form stable compounds with chromium at a wide temperature range, and magnesium chromite ($MgCr_2O_4$) is the predominant chromium species. The effects of chlorine and sulfur on the Mg-based sorbent were also investigated. Figure 5 shows the effect of chlorine on the Mg-based sorbent. As shown, $MgCr_2O_4$ still remains to be the most stable chromium compound in the system even when a significant amount of chlorine is present. Magnesium has stronger affinity to react with chromium than chorine does. On the other hand, when a significant amount of sulfur is present in the system, magnesium is consumed by sulfur and forms magnesium sulfate $MgSO_4$. This trend continues up until around 700 °C, above which magnesium sulfate becomes unstable and the Mg becomes available for chromium to form $MgCr_2O_4$.

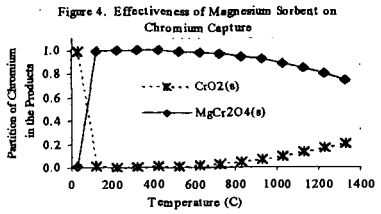


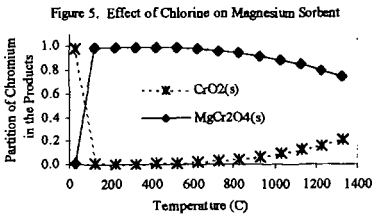

Arsenic-Sorbent and Copper-Sorbent Systems

Calculations were also performed for arsenic and have been reported by Barton and Wu.[18] In short, alkali metals and alkaline earth metals are effective though the performance may be reduced when chlorine or sulfur is present in the system. In addition, aluminum is also effective to capture arsenic. Calculations were not performed for copper due to the lack of thermochemical data for potential compounds between candidate sorbents and copper.

Considering all the modeling results for arsenic and chromium capture, alumina $Al_2O_3$, lime $Ca(OH)_2$, and soda ash $Na_2CO_3$ were chosen to be used in the combustion experiments.

**EXPERIMENT**

The experimental set-up is shown in Figure 6. CCA wood is combusted in a fluidized bed combustor inside the muffle furnace. The hot flue gas is directed into the heat exchanger designed to condense organic matter. The gas stream exiting the heat exchanger enters two columns of absorption spray towers. Each tower is 4 inches in diameter and 2.5 feet in height. The diameter of the column was small enough to achieve good contact between the gas stream and the spraying water without the use of packing materials. Tap water was constantly sprayed from the top of the column and was recirculated until each combustion run finished. The gas streams are further carried into a column of cotton filter to capture the remaining moisture content, volatile matter, and particulate matter in the gas stream. A glass fiber filter was used as the final particulate control device to capture the remaining micron-sized particulate matter. The flow of the gas stream was drawn by a vacuum pump at a flow rate of 30 lpm.

Figure 6: Schematic of Entire Set-Up

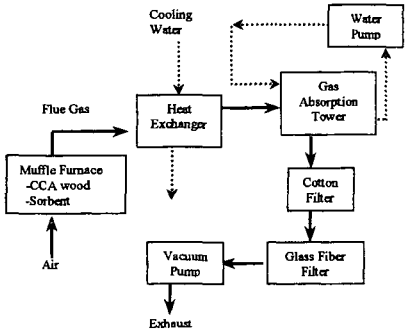


The type of CCA-treated wood combusted was type-C with 2.5 pcf (2.5 lb of chromium copper arsenate per $ft^3$ of dry wood). The wood was processed into sawdust, which was combusted with three different sorbents within a fluidized bed consisting of two layers of stainless steel meshes. 100 g of CCA wood was thoroughly mixed with 18 g of the selected sorbent and placed on the lower stainless steel mesh. Combustion products collected in this layer correspond to the bottom ash in general incineration systems. Another 18 g of sorbent was evenly spread on the upper steel mesh. This layer is designed to capture any vaporizing gaseous metals from the burning of CCA wood in the lower layer. Metals collected in this layer correspond to those observed in the fly ash in general incineration systems. Two sets of experiments were conducted. The experimental conditions are listed in Table 2 below. In the first set, only CCA-treated wood is combusted at three temperatures to establish the baseline. In the second set, three sorbent materials representing different groups (alkali metal, alkaline earth metal, and aluminum-based sorbents) are added to the system to investigate their performance in capturing the metals. After each combustion run, the leaching behavior and the total mass of the metals from the ash is analyzed, according to EPA Method 1311, Toxicity Characteristic Leaching Procedure. Total mass of each of these metals in the ash was analyzed according to EPA Method 3050B, Acid Digestion of Sediments, Sludges, and Soils. Acid Digestion of Aqueous Samples and Extracts for Total Metals for Analysis by FLAA or ICP Spectroscopy. The total mass of these metals in the original CCA sawdust was also analyzed by Method 3050B. Identification of the compounds in the obtained ash is done by X-ray Diffraction (XRD).

Table 2.Experimental Conditions

| | Temperature | Mass of Materials added (g) | | | | |
|---|---|---|---|---|---|---|
| | | CCA Wood | Sorbent | | | Sulfur on Bottom Layer |
| | | | Name | Bottom Layer | Top Layer | |
| Set I | 600 °C | .100g | None | N/A | N/A | 0 g |
| | 750 °C | | | | | |
| | 900 °C | | | | | |
| Set II | 600 °C | 100g | $Al_2O_3$ | 18g | 18g | 0g |
| | | | $Ca(OH)_2$ | 18g | 18g | |
| | | | $Na_2CO_3$ | 18g | 18g | |
| | 750 °C | | $Al_2O_3$ | 18g | 18g | |
| | | | $Ca(OH)_2$ | 18g | 18g | |
| | | | $Na_2CO_3$ | 18g | 18g | |
| | 900 °C | | $Al_2O_3$ | 18g | 18g | |
| | | | $Ca(OH)_2$ | 18g | 18g | |
| | | | $Na_2CO_3$ | 18g | 18g | |

## RESULTS AND DISCUSSIONS

In our preliminary study, four experiments have been conducted at 750°C. For the first run, 100 g of CCA wood was burnt without any sorbent. For the other three runs, 12 g of $Al_2O_3$, $Ca(OH)_2$, and $NaHCO_3$ were individually mixed with 100 g of CCA wood. It took two hours to reach 750°C which was then maintained for 45 minutes. After combustion the obtained ash was analyzed for the leaching behavior of heavy metals and the composition identified. The leaching levels from the TCLP tests are shown in Table 3 and the results from X-ray diffraction for NaHCO3 are given in Figures 7 and 8 (other results are not shown due to space limit).

Table 3: TCLP results for CCA Wood Combustion with and without the Addition of Sorbents.

| | As (mg/L) | Cr (mg/L) | Cu (mg/L) | pH (raw) | PH (TCLP) |
|---|---|---|---|---|---|
| CCA-Only | 87.0 | 16.9 | 23.2 | 6.3 | 2.9 |
| CCA + $Al_2O_3$ | 7.9 | 19.0 | 33.0 | 6.9 | 2.7 |
| CCA + $Ca(OH)_2$ | 0.8 | 84.3 | 1.0 | 12.5 | 11.5 |
| CCA + $NaHCO_3$ | 3687.0 | 4627.0 | 2.1 | 12.6 | 12 |

The TCLP criteria for arsenic and chromium are 5 mg/L. Unfortunately, none of the ash samples passed the TCLP criteria. However, when alumina was added the arsenic leaching was 11 times lower than that without any sorbent (CCA-Only). The calcium based sorbent appears even better. The arsenic concentration drastically decreases to 0.8 mg/L, 110 times lower than the CCA-Only case. Speciation plays an important role here as the solubility varies with speciation. The potential arsenic-sorbent products ($Ca_3(AsO_4)_2$ and $AlAsO_4$) are insoluble.[19] This explains the reduced leaching level observed. Unfortunately, these species were not identified in the XRD.

It is generally known that the pH of the leachate has strong impact on the leaching behavior of heavy metals.[20-21] Warner and Solomon[22] found that copper, chromium, and arsenic were found in the leachate of both new and weathered CCA-treated jack pine, with significantly higher levels of all metals at lower pH values. One interesting phenomenon observed in our results regards this low pH effect on arsenic leaching. Although the pH of the solution after a TCLP test was low (< 3) for both CCA-Only and CCA+$Al_2O_3$, the addition of alumina reduced the leaching of arsenic by 11 times. This comparison proves that addition of alumina reduces the arsenic leaching under aggressive conditions. Dutre and Vandecasteele[23] have observed and also calculated that the addition of lime into a waste fly ash decreases the leaching level of arsenic. However, it is important to emphasize here the distinct difference between the addition of lime before and after the combustion. Lime captures volatile metals during the combustion, which not only reduces the leaching but also reduces the air emission of toxic metals.

Figure 7 X-ray diffractograms of CCA+$Na_2CO_3$ Bottom Ash

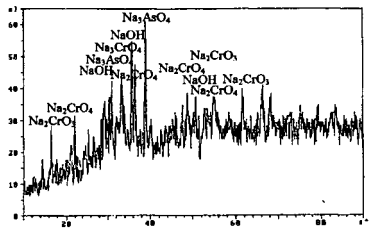


Figure 8 X-ray diffractograms of CCA+Na2CO3 Fly Ash

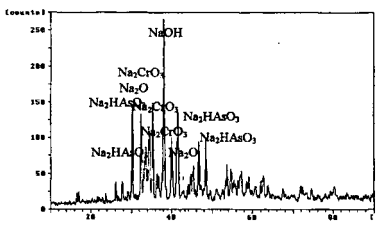


Unfortunately, neither alumina nor lime reduced the leaching of chromium. The cause of this poor result is not clear at this stage. XRD results show that chromium oxide instead of calcium chromite or aluminum chromate is the identifiable component. The result indicates that the sorbent materials are not effective in reacting with the chromium in the system. Mass transfer or reaction kinetics may be the limiting factor.

Leaching of copper was reduced by the addition of lime and sodium bicarbonate. Several studies have shown that copper is known to leach more at low pH.[24,25] The raised pH of the leachate solution most likely caused this low leaching level of copper.

The addition of sodium sorbent such as sodium bicarbonate, on the other hand, caused an incredible amount of leaching. This is due to the formation of very soluble compounds such as $Na_3AsO_4$ and $Na_2CrO_4$ identified by the XRD (Figures 7 and 8). As far as the leaching is concerned, this result is highly undesirable. However, this result can be interpreted in another way. Using these leaching levels of arsenic and chromium, a mass balance calculation was performed to obtain how much of the original amount of these metals in 100 g of wood was still present in the ash. It was found out that at least 78% of arsenic and 88% of chromium still remains in the ash after the combustion. These are very conservative values since these are derived only from a leaching test, not the total metal analysis with an aggressive acid digestion. Typically, only 20~30% of arsenic is reported to stay in the bottom ash. Hence, Na-based sorbent is very effective in retaining arsenic in the bottom ash.

## CONCLUSIONS

CCA-treated wood contains a chemical preservative that consists of arsenic, chromium and copper. The majority of the recycled CCA-treated wood waste is currently burned for energy recovery purposes. There are two major problems associated with the combustion of CCA-treated wood: the emission of heavy metals as gaseous or particulate matter and the leaching of these metals from the ash. Application of sorbent technology may solve these two problems simultaneously.

Thermodynamic equilibrium calculations were performed to predict potential sorbent materials for chemically adsorbing the heavy metals in the CCA-treated wood The results suggest that alumina, alkaline earth metals and alkali metals are effective for capturing both arsenic and chromium. However, alkali metal-based sorbents become less effective when sulfur and chlorine are present in the combustion system. According to these modeling results, alumina, lime and sodium bicarbonate were selected and their performance was examined in an experimental combustion system. The CCA wood sawdust was combusted with three different sorbents within a fluidized bed. TCLP tests were performed on the obtained ash to test the leaching behavior of heavy metals. XRD was performed on the ash sample to identify the products. The addition of alumina and lime greatly reduced the arsenic leaching. None of the sorbents reduced the leaching of chromium. The cause of this poor result is not clear at this stage. Leaching of copper was low when lime or sodium bicarbonate was added as sorbents. This is probably due to the high pH caused by lime and sodium bicarbonate in the leachate. The addition of the sodium sorbent caused an incredibly high leaching level of arsenic and chromium. It was found out that approximately 78% of arsenic and 88% of chromium still remains in the ash after the combustion, showing the sodium sorbent is very effective in retaining arsenic in the ash, which prevents the emission of arsenic.

## ACKNOWDGEMENTS

This research was carried out as a part of the University Scholars Program at the University of Florida. Partial financial supports from the University and the Florida Center for Solid and Hazardous Waste Management are greatly acknowledged. The authors are also grateful to the generous support from Dr. William Wise, Dept. Environmental Engineering Sciences, University of Florida and Dr. R. C. Reynolds, Dept. Mechanical Engineering, Stanford University.

## REFERENCE

1. Solo-Gabriele, H.M. and Townsend, T., **1998**, *Generation, Use, Disposal & Management Options for CCA-Treated Wood, Report #98-1;* FL CSHWM.
2. Solo-Gabriele, H.M., and Townsend, T., **1999**, *Disposal of CCA-treated Wood: An Evaluation of Existing and Alternative Management Options, Report #99-6;* FL CSHWM
3. Mahuli, R.; Agnihotri, S.; Chauk, S.; Chosh-Dastidar, A.; Fan, L.-S. *Environ. Sci. Tech.* **1997**, 31, 3226-3231.
4. Hirata, T.; Inoue, M.; Fukui, Y.; *Wood Sci. Technol.* **1993**, 24, 35-47.
5. Biswas, P.; Wu, C. Y. *J. Air & Waste Manage. Assoc.* **1998**, 48, 113-127.
6. Davison, R. L.; Natusch, D. F. S.; Wallace, K. R.; Evans, C. A. *Environ. Sci. Technol.* **1974**, 8, 1107-1113.
7. Greenberg, R.R.; Zoller, W.H.; Gordon, G. E. *Environ. Sci. Technol.* **1978**, 12, 566-573.
8. Taylor, D. R.; Tompkins, M. A.; Kirton, S. E.; Mauney, T.; Natusch, D. F. S.; Hopke, P.K. *Environ. Sci. Technol.* **1982**, 16, 148-154.
9. Pohlandt, K.; Strecker, M.; Marutzky, R., *Chemosphere* **1993**, 26, 2121-2128.
10. Messick, B.W. Graduate Thesis, University of Florida, **1999**.
11. Uberoi, M.; Shadman, F. *AIChE J.* **1990**, 32, 307-309.
12. Ho, T.C.; Chen, C.; Hopper, J. R.; Oberacker, D. *Combust. Sci. Technol.* **1992**, 85, 101.
13. Gullet, B.K.; Raghunathan, K. *Energy and Fuels* **1994**, 8, 1068-1076.
14. Chen, J.C.; Wer, M.Y. *Environment International* **1996**, 22, 743-752.
15. Brian, I. *Thermochemical Data of Pure Substances*; VCH: Germany, **1995**.
16. Chase, M.W.; Davies, C.A., Downey, J.R.; Frurip, D.J.; McDonald, R.A.; Syverud, A.N.; *JANAF Thermochemical Tables, 3rd Edition*; ACS and AIP for the NBS, Midland, MI, **1986**.
17. Reynolds, W.C. "STANJAN-Interactive Computer Program for Chemical Equilibrium Analysis," Department of Mechanical Engineering, Stanford University, **1995**.
18. Wu, C. Y. and Barton, T., Paper No. 408, *92th Annual Meeting of the Air & Waste Management Assoc.*, St. Louis, MO, June 20-24, 1999.
19. CRC Handbook of Chemistry and Physics. 58th ed., CRC Press, Cleveland, Ohio., **1977**
20. Wasay, S. A. J. *Environ. Sci. Health* **1992** A27(1), 25-39
21. Cooper, P. A. *Forest Products J.* **1991**, 41, 30-32.
22. Warner, J. E.; Solomon, K. R. *Environmental Toxicology and Chemistry* **1990**, 9, 1331-1337.
23. Dutre, V.; Vandecasteele, C. *Environ Sci. Technol.* **1998**, 15, 55.
24. Carey, P. L.; Mclaren, R.G.; Adams, J.M. *Water, Air and Soil Pollution* **1996**, 87, 189-203.
25. Chirenje, T.; Ma, L. Q. *J. Environmental Quality* **1999**, 28, 760-766